

A practical guide to optimization in X10 expansion microscopy

Sven Truckenbrodt^{1,2,3*}, Christoph Sommer³, Silvio O. Rizzoli^{1,2} and Johann G. Danzl³

Expansion microscopy is a relatively new approach to super-resolution imaging that uses expandable hydrogels to isotropically increase the physical distance between fluorophores in biological samples such as cell cultures or tissue slices. The classic gel recipe results in an expansion factor of ~4×, with a resolution of 60–80 nm. We have recently developed X10 microscopy, which uses a gel that achieves an expansion factor of ~10×, with a resolution of ~25 nm. Here, we provide a step-by-step protocol for X10 expansion microscopy. A typical experiment consists of seven sequential stages: (i) immunostaining, (ii) anchoring, (iii) polymerization, (iv) homogenization, (v) expansion, (vi) imaging, and (vii) validation. The protocol presented here includes recommendations for optimization, pitfalls and their solutions, and detailed guidelines that should increase reproducibility. Although our protocol focuses on X10 expansion microscopy, we detail which of these suggestions are also applicable to classic fourfold expansion microscopy. We exemplify our protocol using primary hippocampal neurons from rats, but our approach can be used with other primary cells or cultured cell lines of interest. This protocol will enable any researcher with basic experience in immunostainings and access to an epifluorescence microscope to perform super-resolution microscopy with X10. The procedure takes 3 d and requires ~5 h of actively handling the sample for labeling and expansion, and another ~3 h for imaging and analysis.

Introduction

Super-resolution microscopy, which was introduced to biology around the turn of the millennium, subsumes techniques that can resolve details on a scale finer than the diffraction limit of classic light microscopy (typically 250–300 nm)^{1–5}. Diffraction of light waves sets a lower limit on the smallest spot size to which the light can be focused and causes point-like emitters in the sample to appear as diffraction patterns of finite spatial extent (point-spread functions) when imaged in the microscope. Hence, adjacent fluorophores that are separated by less than about half the wavelength of light cannot be resolved in a conventional light microscope. To overcome this limitation, the most common approaches include coordinate-targeted methods, such as stimulated emission depletion (STED) microscopy^{1,2}, and single-molecule-based methods, such as photo-activated localization microscopy (PALM), stochastic optical reconstruction microscopy (STORM)^{3–7}, and point accumulation for imaging in nanoscale topography (PAINT)^{8–10}. Both types of approaches employ distinguishable molecular states to sequentially read out fluorophores located within a diffraction-limited zone and hence tell them apart. Structured illumination microscopy (SIM) enables a resolution increase of a factor of ~2 with respect to conventional imaging in its linear variant¹¹ and higher factors for nonlinear SIM¹².

Super-resolution imaging has revolutionized biological research in a surprisingly short period of time^{13–17}. It has not only enabled direct visualization of the molecular organization of biological systems and the discovery of biological phenomena that went hitherto unnoticed^{18–27}, but it has also resulted in a rethinking of how to obtain and interpret imaging data. Consequently, improvements in methodology and data analysis, facilitating access to super-resolution technology and furthering collective understanding of super-resolution data, will continue to be strong catalysts for biological discovery. However, biological laboratories that do not specialize in super-resolution imaging are often confronted with three major challenges that limit the further distribution of super-resolution imaging: (i) the requirement for relatively expensive equipment, (ii) the need for highly trained personnel, and (iii) the limited availability of optimized fluorophores with particular photo-physical properties for multicolor super-resolution imaging.

¹Institute of Neuro- and Sensory Physiology, University of Göttingen Medical Center, Göttingen, Germany. ²Center for Biostructural Imaging of Neurodegeneration, University of Göttingen Medical Center, Göttingen, Germany. ³Institute of Science and Technology Austria, Klosterneuburg, Austria.

*e-mail: sven.truckenbrodt@ist.ac.at

Expansion microscopy, introduced in 2015 by the Boyden lab²⁸, is the most recent addition to the super-resolution toolbox and is fundamentally different from STED and PALM/STORM. Whereas STED and PALM/STORM strive to separate fluorophores by increasing optical resolution, expansion microscopy increases the physical distance between them by manipulating the sample itself. The basic idea is to isotropically expand a sample in order to physically increase the distance between the emitters. This means that fluorophores originally located within a diffraction-limited zone in the sample—and whose point-spread functions would therefore be highly overlapping—become sufficiently separated after expansion for their point-spread functions to be distinguished in conventional fluorescence microscopy. The appeal of expansion microscopy is that it may alleviate many of the challenges of classic super-resolution techniques listed above: (i) expansion microscopy is cheap and can be performed on conventional microscopes, (ii) it can be used by anyone with basic training in microscopy and biological laboratory techniques, and (iii) it facilitates comparatively trivial multi-color imaging via the use of standard fluorophores, without the need for special photo-physical properties^{29,30}. Sample expansion is achieved with a swellable hydrogel. The original gel composition enabled approximately fourfold expansion, yielding a resolution of ~70 nm at an expansion factor of 4.5 (Chen et al.²⁸). More recently, a resolution of ~25 nm has been reached with two different approaches. Iterative expansion microscopy³¹ employs two 4× gels sequentially on the same sample, for 10- to 20-fold expansion. By contrast, our recently developed X10 microscopy³² uses a straightforward protocol based on a novel gel chemistry for tenfold expansion in a single step (see Box 1 for gel chemistries).

Although expansion microscopy has thus been quickly adopted by the field^{32–38} and is easy to implement in principle, it is yet a relatively young technique that is still undergoing development and optimization. Numerous factors can influence data quality and reproducibility but may not be immediately apparent. The original expansion microscopy approach adopted procedures from other applications, such as proteolytic digestion with proteinase K or primary amine modification via *N*-hydroxysuccinimide (NHS) chemistry. These procedures have undergone optimization over the 3 years since their introduction to more fully tailor them to the specific requirements of expansion microscopy. We present here a protocol that strives to make clear the underlying principles of expansion microscopy, and in particular X10 microscopy, and their influence on the experimental outcome for novice users. We further summarize recent improvements and suggested optimizations for experienced users. In particular, we strive to provide useful tips on the handling of expansion microscopy gels and data, point out potential pitfalls and their solutions, and discuss several aspects relating to quality control in an effort to increase reproducibility and reliability of results. Our goal is to enable users to make informed decisions and develop their own optimizations when applying expansion microscopy. Although we here focus on X10 microscopy of cultured cells, the guidelines we provide are often applicable to classic fourfold expansion microscopy as well. Table 1 details which protocol sections are specific to X10 and which ones can be equally employed in fourfold expansion and X10 microscopy.

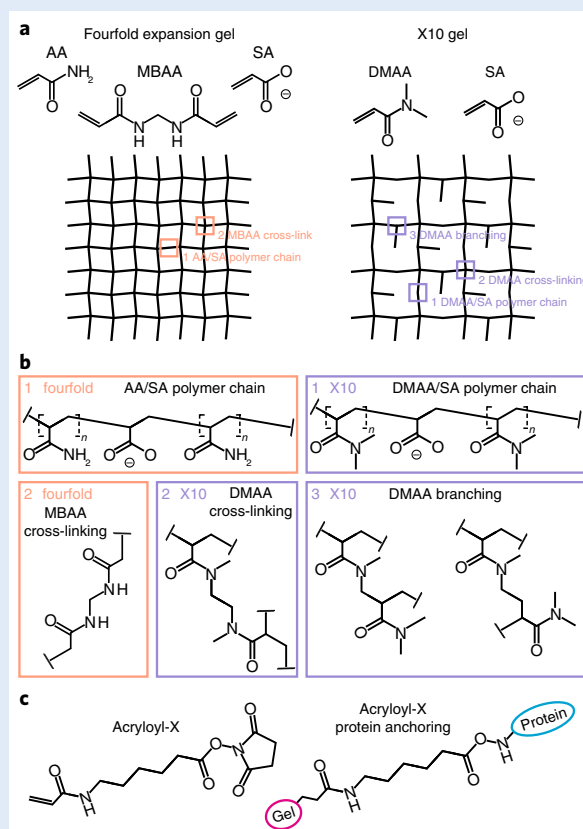
Development of the procedure

The classic expansion microscopy protocol²⁸ was developed in the Boyden lab in 2015. It is based on the well-known property of some acrylate polymer gels to expand in deionized water, which inspired the Boyden lab to suggest exploiting this phenomenon as a way to increase effective resolution in microscopy. They implemented a gel chemistry that resulted in a fourfold expansion of biological samples. Since then, the most substantial practical improvement over the original procedure was to replace the original, rather cumbersome, DNA-oligo-based anchoring with direct anchoring of proteins to the gel, which was achieved almost simultaneously in 2016 by the Vaughan lab³³ and the Boyden lab³⁵. The first approach to further increase the expansion factor, and therefore resolution, was again introduced by the Boyden lab, in 2017, in the form of iterative expansion microscopy, in which an additional fourfold expanding gel is applied after the first fourfold expansion gel, resulting in a multiplication of the expansion factors provided by each of the gels, with handover of fluorophores between the gels through DNA oligos³¹. We recently described the first improvement to the expansion factor of the gel itself by adapting a different gel chemistry³⁹ (Box 1) for X10 microscopy, resulting in an increase of the expansion factor to approximately tenfold³²; this is compatible with direct protein anchoring and does not require DNA-oligo-based labeling or complex handover procedures for probes.

Box 1 | Expansion microscopy gel chemistry

Expansion microscopy utilizes hydrogels that can swell to several-fold their initial volume when placed in ddH₂O^{65,66}. This occurs when water molecules interact with the hydrophilic ionic side groups of the gel. Gels with more ionized groups thus usually attain higher expansion factors^{67,68}. The second parameter affecting the expansion factor is the number of cross-links in the gel: fewer cross-links usually permit a higher expansion factor but at the same time lower the stability of the gel^{67,68}. Hydrogels can often take up many times the weight of the polymer itself in water, resulting in gels that are stable with >99.9% water content by weight in the fully expanded state. The integrity of the expanded hydrogel is maintained by covalent cross-links between the monomer components used to form the polymer. The maximum useful attainable expansion factor of a hydrogel for expansion microscopy thus depends on finding gel recipes that provide few enough cross-links in a matrix with many ionic groups to attain a high expansion factor, but enough cross-links to retain stability of the gel during handling and imaging³⁹.

In classic fourfold expansion microscopy, the hydrogel is composed of sodium acrylate (SA), acrylamide (AA), and *N,N'*-methylenebisacrylamide (MBAA). The polymerization of these monomers is initiated by ammonium persulfate (APS) and is accelerated by tetramethylethylenediamine (TEMED). AA provides the backbone of the gel meshwork, MBAA is used as a cross-linker (see the figure below). As both AA and MBAA are nonionic, SA is added to provide ionic groups for swelling. This results in a gel that can increase ~30- to 90-fold in volume when placed in ddH₂O²⁸.



In X10 expansion microscopy, the hydrogel is composed of SA and *N,N*-dimethylacrylamide (DMAA). The polymerization of these monomers is initiated by potassium persulfate (KPS) and accelerated by TEMED. DMAA provides both the backbone of the gel and the cross-links here, as it is self-cross-linking when catalyzed with KPS (see the figure above). However, DMAA is also nonionic, and thus SA again is added to provide ionic groups for swelling. This results in a gel that can increase up to ~1,000-fold in volume when placed in ddH₂O³². The expansion factor of the resulting gel also depends on the molar ratio of DMAA to SA: more SA provides more ionic groups, but this approaches a plateau at a DMAA/SA molar ratio of 80:20, and higher amounts of SA relative to DMAA can also compromise gel integrity, as more positions in the matrix are occupied by SA, leaving fewer cross-links formed by DMAA³⁹.

The figure above shows the expansion gel chemistry. Panel **a** depicts the components and schematics of the classic fourfold expanding gel and of the X10 gel for expansion microscopy. The gel patterns shown do not necessarily reflect the periodicity or probability of these in the final polymer. These are purely intended as nonquantitative visual guides to differentiate the X10 gel from the fourfold expanding gel, as the precise organization of the X10 gel as well as that of the fourfold expanding gel are currently unknown. In panel **b**, the structure of the polymer chain and its cross-links are given. For the fourfold gel, the components are SA, MBAA, and AA. SA is depicted here in its ionized form, with the Na⁺ ion dissociated from the carboxylate group. SA and AA form linear polymer chains, which can be cross-linked by MBAA. Both reactions require the creation of radicals at the ethylene groups of SA, AA, and MBAA through ablation of an electron by APS as initiator (not depicted). For the X10 gel, the components are SA and DMAA. SA is again depicted in its dissociated form. DMAA and SA can form linear polymer chains, but DMAA can also react in alternative ways, in which KPS creates radicals through electron ablation, not at the ethylene group, but at one of the methyl groups. These radicals can then either attack another methyl group, leading to cross-linking, or another ethyl group, leading to different forms of branching. Note that the couplings highlighted here are only exemplary structures from the gel, based on likely radical reaction behavior. The outcomes of radical-based polymerization reactions are difficult to predict. Other reactions, omitted for simplicity, are also plausible. Acryloyl-X is used in both gel variants to anchor proteins to the gel (see panel **c**). Acryloyl-X is bifunctional: it contains a succinimidyl group that can covalently attach to primary amines of proteins via NHS chemistry, and it contains an AA group at the opposite end that can integrate into the growing gel matrix in place of AA or DMAA.

Table 1 | Applicability of protocol stages to expansion microscopy techniques

Protocol stage	Steps	Applicable to
Labeling	1–8	Any immunolabeling-based expansion microscopy
Anchoring	9–11	Any immunolabeling-based expansion microscopy
Polymerization	12–20	X10 expansion microscopy
Homogenization	21–23	Any immunolabeling-based expansion microscopy
Expansion	24 and 25	Any immunolabeling-based expansion microscopy
Imaging	26–30	Any immunolabeling-based expansion microscopy
Validation	31 and 32	Any immunolabeling-based expansion microscopy

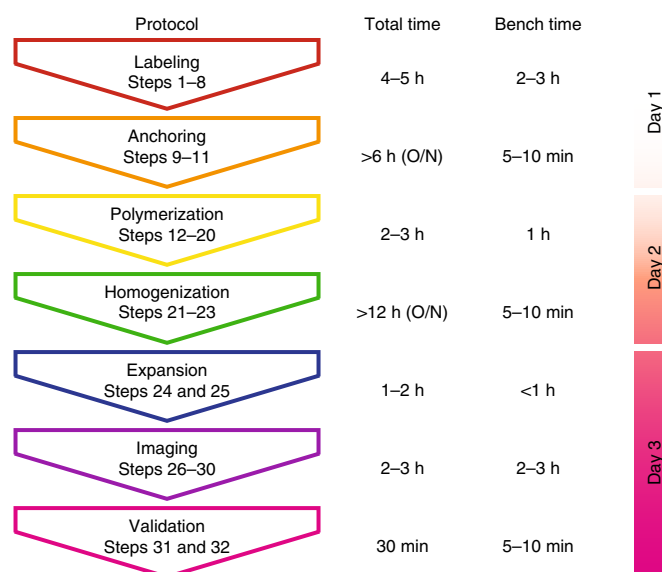


Fig. 1 | Outline and timing of the X10 expansion microscopy protocol. For each stage of the protocol, the corresponding steps of the Procedure are noted in the 'Protocol' column. The entire protocol, from the unfixed sample to post-expansion imaging, requires 3 d. This consists mainly of incubation time, reflected in the 'Total time' column for each step. The actual time spent at the bench, microscope, or computer is considerably less and is given in the 'Bench time' column. On day 1, labeling and anchoring are performed. On day 2, gel polymerization and homogenization take place. On day 3, the sample is expanded, imaged, and validated. O/N, overnight.

Overview of the procedure

Expansion microscopy consists of a seven-stage procedure^{28,29,32} (see Fig. 1 for a schematic overview): (1) labeling, (2) anchoring, (3) polymerization, (4) homogenization, (5) expansion, (6) imaging, and (7) validation. Stages 2–6 constitute the experimental part of expansion microscopy per se. Stages 1 and 6 are adapted from common and established procedures. Stage 7 addresses issues relating to reliability and reproducibility of data peculiar to expansion microscopy and should be included in any expansion microscopy experiment. In particular, the expansion factor and possible distortions must be evaluated. Below, we describe these stages in more detail.

- 1 Labeling (Steps 1–8).** Labeling can be performed by immunostaining^{28,32,33,35,40}, RNA FISH^{40–42}, DNA FISH³⁴, or, for the 4× gel and after optimization, expression of fluorescent proteins³⁵. In situations in which fluorescent proteins cannot be visualized directly due to loss of fluorescence during the expansion protocol, they can alternatively be detected via immunostaining. The immunostaining can be performed by following common and established protocols. Expansion microscopy per se is simply added after the immunostaining is completed^{29,33,35}.
- 2 Anchoring (Steps 9–11).** Anchoring is the process of preparing the sample in a way that allows a covalent cross-linking between imaging probes introduced during immunostaining and the expansion gel itself. It is necessary to couple probes into the gel to prevent loss of fluorophores and

to conserve their relative positions during expansion. Originally, this was achieved via DNA-oligo-coupled antibodies. These were detected by complementary DNA oligos that carried a reactive acrylate group, for anchoring the DNA oligo to the gel matrix, and a fluorophore, for detection²⁸. This procedure has been largely superseded by more direct protein anchoring via a chemical agent, Acryloyl-X³⁵ or MA-NHS³³, that directly reacts with proteins via NHS chemistry and also integrates into the gel matrix via an additional acrylate group (Box 1). Acryloyl-X is used here, but the two compounds are interchangeable. This principle has been adapted to RNA retention as well⁴².

- 3 *Polymerization (Steps 12–20)*. A gelation solution of monomers is cast across the sample. The monomers are then allowed to polymerize into a swellable hydrogel, integrating the anchored targets.
- 4 *Homogenization (Steps 21–23)*. Homogenization is necessary to prepare the sample for expansion by disrupting its mechanical structure. If this step is insufficiently stringent, the sample can distort or rupture because of the opposing forces of tissue cohesion and expansion. Homogenization is most commonly achieved using the promiscuous proteolytic enzyme proteinase K (as in this protocol); heat denaturation is a recently described alternative³⁵.
- 5 *Expansion (Steps 24 and 25)*. After homogenization, the gel is expanded several-fold over its original volume by placing it in ddH₂O. Expansion is achieved by washing out ions from the gel matrix that maintain the gel in a constricted conformation through ionic interactions. We discuss the original gel recipe used to achieve an expansion factor of approximately fourfold²⁸ and provide our recently developed X10 microscopy recipe to achieve an approximately tenfold expansion by using an alternative gel chemistry^{32,39} (Box 1).
- 6 *Imaging (Steps 26–30)*. Imaging can be performed on any available fluorescence microscope using, for example, epifluorescence microscopy^{28,32}, confocal microscopy^{28,35}, light-sheet microscopy^{42,43}, SIM^{38,44,45}, STED microscopy^{46,47}, STORM microscopy⁴⁸. In this protocol, we exemplify our approach by imaging on an epifluorescence microscope to demonstrate its compatibility with more conventional equipment.
- 7 *Validation (Steps 31 and 32)*. We discuss how to address two important issues that are specific to expansion microscopy and that can cause errors in data interpretation: expansion factor and distortions.

The protocol we present here focuses on the most widely used imaging application, antibody-based immunostainings, and elaborates on the experimental details of each step, including the pitfalls associated with them. We have successfully used our X10 approach on cultured cell lines, primary neuronal cell cultures, and cryo-sectioned brain tissue slices, and we expect that it can be used for any type of cultured cell line or primary cell culture and other types of tissue slices after sample-specific optimization similar to the development the original 4× gel has undergone over time. We strive to enable users to critically evaluate each step of the procedure, and to make informed decisions on which approach to use or which optimizations to pursue for their own samples. Our protocol includes recent improvements over and suggested optimizations of the original protocols for expansion microscopy and details where it is helpful to apply them, either in the X10 or in the fourfold expansion setting.

Applications of the method

A wide array of applications have been demonstrated for expansion microscopy. The classic fourfold expansion protocol has been successfully applied for imaging based on protein immunostainings in a variety of different samples: 2D cell culture^{28,31,33,35,42}, brain tissue slices^{28,31}, other tissue slices³⁵, zebrafish³⁷, *Drosophila*^{36,38,43}, microorganisms⁴⁴, and clinical samples³⁴. Recently, whole *Drosophila* brains have been imaged with this technique⁴³. Related techniques also relying on the expansion of gels have been used to investigate other whole isolated organs: MAP⁴⁹ and CUBIC-X⁵⁰. The recent X10 protocol has been demonstrated in 2D cell culture and brain tissue slices, with applications in other tissue samples awaiting further optimization³². Expansion microscopy has further been demonstrated for super-resolution imaging of fluorescent protein-labeled samples^{28,35}, DNA³⁴, and RNA⁴², including RNA multiplexing in MERFISH⁴¹.

Modifications and optimizations have been introduced for each of the specific samples and applications cited above. Specialized protocols have also been developed to preserve fluorescent proteins³⁵. Conserving the fluorescence capability of fluorescent proteins, however, so far appears to be largely incompatible with the strong homogenization required when large expansion factors are

attained, such as in X10 microscopy³², as thorough proteolytic digestion or other forms of denaturation also largely abolish the fluorescence capability of fluorescent proteins. In such cases, fluorescent proteins can easily be visualized via antibodies.

Limitations

General considerations for super-resolution microscopy

To obtain a faithful representation of the sample, three requirements must be met by any super-resolution approach. (i) The gross, and in particular the nanoscale structure, must be adequately preserved during sample preparation. Adequate care must hence be taken when optimizing fixation conditions for the chosen imaging targets. We give some specific examples in the Procedure. (ii) To fully visualize a biological structure in a fluorescence image, it must be adequately spatially sampled with fluorophores, i.e., the labeling density must be sufficiently high. This requirement is considerably more stringent in super-resolution microscopy, including expansion microscopy, than in diffraction-limited microscopy. With insufficient labeling density, structures that are known or assumed to be continuous, e.g., microtubules, may develop a ‘patchy’ or ‘spotty’ appearance in super-resolution imaging, whereas the same labeling density would be adequate for the same structures and appear continuous at the lower spatial resolution of conventional wide-field or confocal microscopy⁵¹. Insufficient labeling density would thwart any effort to decode an unknown structure by increasing spatial resolution. (iii) The imaging approach must provide the warranted spatial resolution.

Linkage error

When the resolution approaches the size of the labeling probes (usually primary/secondary antibody complexes with a spatial extent of 15–20 nm^{51–53}), imaging artifacts caused by the probe displacement (the so-called linkage error) limit the usefulness of an increased resolution. This is a problem that affects all super-resolution techniques equally^{13,52}. Evidently, with the increased resolution of X10 microscopy approaching the spatial scales of target-to-probe displacements, this issue is more pressing than in classic fourfold expansion microscopy. Analogous considerations concerning increased spatial resolution hold for spatial sampling and image brightness.

Spatial sampling

As highlighted above, all super-resolution imaging techniques, expansion microscopy included, suffer in the case that labeling density is insufficient. If a sample structure provides problems for access of probes, such as access of antibodies to tightly packed macromolecular complexes, steric hindrance can result in imaging artifacts from insufficient epitope coverage⁵¹. Such incomplete labeling becomes apparent only when the resolution is high enough to resolve the gaps between sparse labels, so the higher the attained resolution, the more acute this problem becomes.

Achievable expansion factor and resolution

The resolution improvement of expansion microscopy, as compared with that of non-expanded samples imaged on the same setup, directly corresponds to the expansion factor^{28,31,32}. This means that the main limitation of resolution in expansion microscopy is the expansion factor that can be achieved with the hydrogel used. Recently, this has been improved from approximately fourfold²⁸ to tenfold³². Tenfold expansion might represent the current limit of acrylate-based hydrogels³⁹, but a further increase in the future, using improved gel chemistries, is probable. Iterative expansion microscopy is an elegant stepwise expansion of a sample through the iterative application of several gels to multiply their individual expansion factors³¹. The investigation of the applicability of this approach to gel recipes different from that of the original fourfold gel has only just begun, but it shows promise⁴³. The trade-offs are that iterative expansion requires a more complex DNA-oligo-based labeling and is considerably more expensive and time-consuming³¹. The resolution attained through iterative expansion microscopy of the classic 4× gel equals that of single-step X10 microscopy^{31,32}. Because expansion occurs in all three dimensions, z-resolution is increased by the expansion factor as well. However, the increase in sample thickness can also cause issues with imaging depth and optical aberrations^{46,54}. Although the sample is cleared during homogenization, and light transmittance issues usually associated with imaging of thick biological specimens are thus less of a concern, most high-magnification objectives have a rather short working distance, potentially making it impossible to image through thicker tissue sections. To avoid optical aberrations, most notably spherical aberrations seen when imaging deep in the sample, the refractive index for which the

objective lens is designed and that of the sample should be matched. Optical aberrations can thus be reduced by using water-immersion objectives or matching the refractive index of the gel sample to oil immersion by incubating the gel in a sucrose solution⁴⁶; this approach, however, typically also results in a slight shrinkage of the gel.

Image brightness

A general challenge in expansion microscopy is the reduced brightness of the samples after expansion. This is due to three factors: (i) certain fluorophores can be damaged during gel polymerization, (ii) dyes can be lost after proteolytic digestion, and (iii) dyes are diluted during expansion in all three spatial dimensions. Some fluorophores are entirely incompatible with expansion microscopy, e.g., because of the presence of diene groups in their chemical structures, which are attacked by the radical gel chemistry during polymerization, leading to essentially complete loss of fluorescence^{28,32,35}. Notably, this affects all cyanine dyes³⁵, including Alexa Fluor 647. However, using fluorophores mostly resistant to the polymerization reaction may still result in reduced brightness. Fluorophores may be partially lost through chemical damage during the radical reactions occurring during gel polymerization^{28,35}. Furthermore, the random nature and incomplete efficiency of the anchoring and homogenization procedures necessarily leads to the loss of an unknown fraction of fluorophores from the sample. All fluorophores attached to a proteolytically created protein fragment that was not also covalently linked to the gel matrix during anchoring undergo this fate. Increased demands on mechanical homogenization in X10 microscopy relative to classic fourfold expansion may exacerbate fluorophore loss such that additional care has to be taken. Last, but not least, the number of fluorophores per voxel is diluted through the isotropic expansion of the sample in all three dimensions by a factor that equals the expansion factor to the power of three ($4^3 = \sim 64$ -fold reduction for classic fourfold expansion microscopy, and $10^3 = \sim 1,000$ -fold reduction for X10 microscopy). A number of post-expansion signal amplification procedures have been suggested^{31,38,45}. First, there are approaches that rely on DNA-based reactions to produce additional binding sites for cDNA oligos coupled to fluorophores³¹. However, these are relatively complex and expensive reactions, and might degrade effective resolution through shrinkage of the gel in the reaction buffer and also through an increased linkage error due to a further displacement of the probes from the epitope. Second, there are approaches based on post-expansion immunostainings, in which either only the secondary antibody or both the secondary and the primary antibodies are applied after expansion^{38,45}. The potential downside of these approaches is that not all epitopes are guaranteed to be preserved after homogenization. This could be a particular problem for samples that require extensive proteolytic digestion to prevent distortions or ruptures during expansion (e.g., tissue slices).

Mechanical properties of the sample

Possibly the greatest caveat of expansion microscopy is that the sample is altered structurally when its volume is increased by a factor of 64- to 1,000-fold. This is an unusually drastic manipulation of a sample during preparation for imaging and can introduce distortions or ruptures. It should be noted, however, that distortions or ruptures are also relatively common during sample preparation for standard (immuno-)stainings for light microscopy or during sample preparation for electron microscopy; such distortions result from fixation, permeabilization, sectioning, and general sample handling. Steps should be taken to minimize these issues, and different samples react differently to manipulation. As a rule of thumb, mechanically more tough or inhomogeneous samples (such as tissue slices, whole organisms such as *Drosophila* larvae, or dense multilayered cell cultures) will pose greater challenges in expansion microscopy than mechanically less tough and more homogeneous samples (such as single-layered cell cultures, many unicellular organisms, or protein complexes *in vitro*). This means that optimization in sample preparation needs to undergo further development for expansion microscopy, and the particularities of any new sample must be considered individually.

Distortions and ruptures

Each imaging approach strives to achieve a faithful representation of the sample. Apart from fluorophore loss, distortions during the expansion process represent the most critical issue that might jeopardize the fidelity of the imaging process. The degree of distortions in the diffraction-limited spatial range can easily be quantified for each sample by comparing pre- and post-expansion images (see Step 32 of the Procedure), and upper bounds to nanoscale distortions can be inferred from comparison with other super-resolution methods. Although a range of different mechanisms may plausibly lead to distortions, no experimental data exist that quantify the contribution of an

individual mechanism. They include the following: (i) in principle, distortions may be caused by inhomogeneities of the polymerized gel itself, caused, e.g., by local interactions with the sample structure or residual moisture during polymerization, thus influencing the local nano- or micro-architecture of the gel. (ii) As discussed above, mechanical toughness of a sample can sometimes become a problem. In the worst case, when homogenization is insufficient, this can lead to a distorted or even ruptured sample. The reason for this is a ‘tug-of-war’ between the sample, which strives to remain in its original size, and the gel, which strives to expand. If this is the case, specifically optimized mechanical homogenization procedures are required. For example, classic fourfold expansion microscopy became applicable to *Drosophila* larvae, which have a very tough chitin cuticle, only after a three-tiered 7-d homogenization with chitinase, collagenase, and proteinase K³⁶. With its increased expansion factor, X10 microscopy relies more heavily on effective mechanical homogenization than fourfold expansion. Accordingly, classic homogenization of 2D cell cultures with proteinase K for a few hours at 37 °C, sufficient for the classic 4× gel²⁸, proved insufficient for the X10 gel and resulted in ruptures in dissociated neuronal cultures³², even though the mechanical toughness of dissociated cell cultures is weak compared to that of tissue slices. Similarly, although X10 microscopy has been demonstrated on brain tissue slices, expansion of other tissue samples will require further optimization. (iii) A similar effect is observed with insufficient anchoring, which in combination with residual cohesion of the sample may also lead to distortions and localized rupture of mechanically loaded anchoring points. All three mechanisms may potentially lead to distortions or, if sufficiently severe, to large-scale ruptures of the expanded sample. Therefore, strategies aimed at reducing distortions will often follow the same lines as strategies to avoid sample ruptures.

Fluorescent proteins

Fluorescent proteins are poorly preserved with standard proteinase-based homogenization methods^{28,32}, as they are also targeted by the proteases. The degree of preservation of fluorescence depends on the nature of the fluorescent protein³⁵, but fluorescence decline generally becomes more severe during harsher homogenization³² and often results in essentially complete loss of signal. Although dedicated protocols for fluorescent protein preservation have been developed for fourfold expansion³⁵, the thorough mechanical homogenization we apply here for X10 microscopy to accommodate the increased expansion factor is not compatible with fluorescence emissions from green fluorescent protein and its kin. This issue can be circumvented by antibody tagging of the fluorescent proteins, allowing the use of established fluorescent protein-labeled experimental systems in expansion microscopy, and in particular in X10 microscopy. Note, however, that fluorescent proteins cannot always be identified by a specific antibody when used in conjunction with similar fluorescent proteins. For example, GFP, YFP, and CFP, derived from the same protein, share a very high sequence homology, and are thus so similar that GFP antibodies typically also recognize YFP and CFP.

Limitation to fixed samples

Finally, owing to the principle of operation (fixation and homogenization required), all expansion microscopy approaches are incompatible with live-cell imaging.

Experimental design

Expertise and equipment needed to implement the protocol

The requirements in personnel training and equipment for implementing protein-immunostaining expansion microscopy, as detailed in this protocol, represent very low hurdles compared to those of other super-resolution techniques. Any laboratory or scientist trained in basic immunostaining and with access to fluorescence imaging should be able to implement the technique. Expansion microscopy can be added as an extension to any standard immunostaining and fluorescence-imaging procedure. However, we do strongly encourage taking into account the higher demands in terms of labeling and structural preservation that are inherently linked to the increased spatial resolution and that hence apply to all super-resolution methods^{13,55–57}.

Optimization for different samples

Expansion microscopy is still a relatively young technique, and optimizations continue to emerge. The main need for optimization arises from a combination of two factors: increased expansion factors of newly introduced gel recipes, and differences in the mechanical toughness of samples on which expansion is performed. Applying expansion microscopy to a new type of sample inevitably requires

Table 2 | Optimizations and when to apply them

Optimization	Effect	Apply when	Do not apply when
Anchoring in sodium bicarbonate buffer at pH 8.3 instead of in PBS at pH 7.0–7.5	This should improve the efficiency of the NHS-based anchoring reaction of Acryloyl-X to primary amines in the sample	-The signal is weak after expansion (improved anchoring can retain more fluorophores) -Distortions are prevalent after expansion (improved anchoring should more densely link the sample into the gel)	Retention of free primary amines after polymerization is desired for some experimental reason (e.g., some reaction to be performed after expansion)
Homogenization in adjusted digestion buffer (with Ca^{2+}) instead of in classic digestion buffer (without Ca^{2+})	Proteinase K does not rely on Ca^{2+} ions for catalyzing proteolysis, but Ca^{2+} ions improve the stability of proteinase K	-Ruptures are prevalent after expansion (improved digestion will reduce the mechanical resistance offered by the sample during expansion) -Digestion time is long, e.g., overnight (proteinase K will lose stability over the course of a few hours and thus become inactive, making longer digestion times ineffective in further improving homogenization)	The signal is weak (increased digestion reduces retention of fluorophores, as cuts in the peptide chains are more frequent and thus fragments will become smaller, reducing the probability of retaining fluorophores anchored to the remaining pieces)

adaptation of the methodology to the specifics of the sample. We focus on cultured cells, and for the steps in the Procedure dealing with polymerization (Steps 12–20), we provide instructions specific to the X10 methodology. The other steps can be adopted in classic fourfold expansion microscopy as well, where the same considerations concerning optimizations also hold, as detailed in Table 1. Further guidance on when to apply which optimization is provided in Table 2.

This guide is intended to give practical advice for such optimizations, including some suggestions for how to alter critical parameters of the expansion microscopy procedure. In particular, we point out some modifications to anchoring and homogenization approaches in the Procedure. To give new users a firm basis for developing optimizations of their own, the descriptions given in this protocol also include some detailed considerations on which reactions occur during each step, how they occur, and how they might be optimized to improve the outcome.

Quality control of expanded samples

This guide also provides some practical advice for quality control of expanded samples (Steps 31 and 32). Drastic damage to a sample after expansion is usually obvious. However, the evaluation of distortions in morphologically well-preserved samples is often not trivial. Yet, careful validation of the generated results, including expansion factor and distortions, is an absolute necessity for expansion microscopy to serve as a reliable and valuable tool for super-resolution imaging. Here, we also provide an easy-to-use automated analysis script (Supplementary Data 1), based on the basic Python Anaconda suite, to facilitate and streamline this process for nonexpert laboratories.

Modularity of the approach

One advantage of expansion microscopy is that it is a highly modular method, and improvements to one of its seven stages can usually be combined with optimizations performed independently for any other stage. For example, improvements to the homogenization of 2D cell cultures developed for X10 can be used with the classic 4× gel. Similarly, developments in homogenization procedures for tissue slices can also improve homogenization of 2D cell cultures, and so on. Because the polymerization procedure for classic fourfold expansion microscopy itself has been detailed and improved in many previous publications^{28,31,33,35,40,45}, and to keep the protocol concise, we focus here on the more recent X10 technique in the section of the Procedure where we deal with polymerization. However, all information presented in the other six stages of the protocol is equally applicable to the 4× gel or other variants of expansion microscopy, as long as the potential trade-offs we discuss are taken into account. Table 1 summarizes the stages of the protocol from which advice can be also applied to expansion microscopy techniques other than X10.

Combining X10 with advanced imaging platforms

One important advantage of expansion microscopy is the fact that, although it uses conventional diffraction-limited microscopy equipment, it is capable of delivering effective spatial resolution that

corresponds to diffraction-unlimited microscopy^{28,31,32}. An *xy*-resolution of 60–80 nm for classic fourfold expansion microscopy²⁸, or 25 nm for X10 microscopy³² and iterative expansion microscopy³¹, can easily be achieved with basic epifluorescence microscopes. The *z*-resolution is limited to ~200 and ~80 nm, respectively, on such setups. However, imaging of expanded samples has been performed on a variety of microscopes, thus combining the benefits of sample expansion with the characteristic features of the respective microscope technology. Clearly, such combinations also require access to the relevant microscopes and the pertinent expertise. Although conventional wide-field microscopes enable super-resolution imaging based on expansion microscopy, they do not provide optical sectioning. Image quality is hence potentially compromised by reduced signal-to-background ratio due to out-of-focus fluorescence. The *z*-sectioning can be improved by using confocal³² or light-sheet microscopes^{42,43}. Here, light-sheet fluorescence microscopy is attractive because it makes optimum use of the photon budget by illuminating only the plane to be imaged and, as a camera-based wide-field approach, it enables high imaging speeds. The resolution attained through expansion microscopy can be further improved by a factor of 2–10 by combination with classic super-resolution techniques such as SIM^{38,44,45}, STED microscopy^{46,47}, or STORM⁴⁸.

Materials

Biological materials

- Cells of interest. We exemplify our protocol here using primary hippocampal neurons from rats (Wistar, P1–P2, mixed sex), cultured as described previously^{58–60}. We anticipate that the protocol can be used with any cultured cell line or primary cells of interest³². **! CAUTION** If you wish to use cell lines, they should be regularly checked to ensure that they are authentic and are not infected with mycoplasma. **! CAUTION** Any research involving animal experimentation must conform to relevant national and institutional regulations. By EU and Austrian law, no specific ethics approval is necessary for terminal organ extraction, as performed here for obtaining primary hippocampal neuron cultures from rats. Follow the relevant regulations in your area.

Reagents

- 6-((Acryloyl)amino)hexanoic acid, succinimidyl ester (Acryloyl-X, SE; Thermo Fisher Scientific, cat. no. A-20770)
- NaCl (Sigma-Aldrich, cat. no. S7653)
- KCl (Sigma-Aldrich, cat. no. P9333)
- KH₂PO₄ (Sigma-Aldrich, cat. no. P9791)
- Na₂HPO₄ (Sigma-Aldrich, cat. no. 71643)
- NaHCO₃ (Sigma-Aldrich, cat. no. S5761)
- NH₄Cl (Sigma-Aldrich, cat. no. A9434)
- CaCl₂ (Sigma-Aldrich, cat. no. C5670)
- Dimethyl sulfoxide (DMSO; Thermo Fisher Scientific, cat. no. D12345)
- NaOH (Sigma-Aldrich, cat. no. 221465)
- Glucose (Sigma-Aldrich, cat. no. G7021)
- MgCl₂ (Sigma Aldrich, cat. no. M8266)
- Borohydride (Sigma Aldrich, cat. no. 213462)
- Glycine (Sigma Aldrich, cat. no. 50046)
- N₂ gas (Westfalen Austria, cat. no. A00340110)
- Argon (Westfalen Austria, cat. no. A00540110)
- Liquid nitrogen (N₂; Westfalen Austria, cat. no. A003415)
- Sodium citrate (Sigma Aldrich, cat. no. 71497)
- Sodium azide (NaN₃; Sigma-Aldrich, cat. no. 71289) **! CAUTION** Sodium azide is acutely toxic, a health hazard, and dangerous to the aquatic environment. Wear appropriate protective equipment and work under a fume hood.
- Sodium acrylate (SA; Sigma-Aldrich, cat. no. 408220) **! CAUTION** Sodium acrylate is dangerous to the aquatic environment. Wear appropriate protective equipment and work under a fume hood. **▲ CRITICAL** We recommend checking the purity of SA whenever a new batch is opened, by making a 0.38 g/ml stock and evaluating the color. If the solution has a strong yellow tint, discard the batch and open a new one, as polymerization is strongly negatively affected by use of impure SA. We recommend storing SA at –20 °C in a desiccated environment to preserve stability, and to regularly repeat the test

of purity (e.g., every 4 weeks) until the batch is used up. SA can usually be stored for up to 6 months (unless the regular purity test is negative).

- *N,N*-dimethylacrylamide (DMAA; Sigma-Aldrich, cat. no. 274135) **!CAUTION** *N,N*-dimethylacrylamide is corrosive and acutely toxic. Wear appropriate protective equipment and work under a fume hood.
- Potassium persulfate (KPS; Sigma-Aldrich, cat. no. 379824)
- *N,N,N',N'*-tetramethylethane-1,2-diamine (TEMED; Sigma-Aldrich, cat. no. T7024) **!CAUTION** *N,N,N',N'*-tetramethylethane-1,2-diamine is flammable and corrosive. Wear appropriate protective equipment and work under a fume hood.
- Tris(hydroxymethyl)-aminomethane (TRIS; AppliChem, cat. no. A3452)
- 2-(*N*-morpholino)ethanesulfonic acid (MES; Sigma-Aldrich, cat. no. M0164)
- EDTA (Sigma-Aldrich, cat. no. EDS)
- Triton X-100 (Sigma-Aldrich, cat. no. 93426) **!CAUTION** Triton X-100 is corrosive and acutely toxic to the aquatic environment. Wear appropriate protective equipment and work under a fume hood.
- Guanidine HCl (Sigma-Aldrich, cat. no. G4505)
- Proteinase K (Sigma-Aldrich, cat. no. P4850) **▲CRITICAL** Proteinase K is available from multiple suppliers, but the activity and stability vary. We had the best experiences with the product cited here.
- Double-distilled water (ddH₂O; Milli-Q Reference Wasseraufbereitungssystem; Merck Millipore, cat. no. Z00QSV0WW)
- Paraformaldehyde (PFA; Sigma-Aldrich, cat. no. 158127) **!CAUTION** Paraformaldehyde is a carcinogen. Wear appropriate protective equipment and work under a fume hood.
- Glutaraldehyde (Sigma-Aldrich, cat. no. G7651) **!CAUTION** Glutaraldehyde is a carcinogen. Wear appropriate protective equipment and work under a fume hood.
- Methanol (Honeywell Research Chemicals, cat. no. 603-001-00-X) **!CAUTION** Methanol is flammable and acutely toxic. Wear appropriate protective equipment and work under a fume hood.
- BSA (AppliChem, cat. no. A1391)
- Low-melt agarose (Roth, cat. no. 6351)
- Primary antibodies used here: anti-synaptophysin (Synaptic Systems, cat. no. 101 004), anti-Bassoon (Enzo, cat. no. SAP7F407), and anti-Homer 1 (Synaptic Systems, cat. no. 160 003)
- Secondary antibodies used here: donkey anti-guinea pig conjugated to Alexa Fluor 488 (Dianova, cat. no. 706-545-148), goat anti-rabbit conjugated to Alexa Fluor 546 (Thermo Fisher Scientific, cat. no. A-11035), and donkey anti-mouse conjugated to CF633 (Biotium, cat. no. 20124)
- Ice (Flockeneisbereiter; Kaelte-Berlin, cat. no. AF 103 AS)

Equipment

- Square plastic tray (245 mm; Nunc, cat. no. 240835)
- Two-component dental silicon (Picodent, Twinsil 22)
- Aluminum foil (Korff, cat. no. KOAF1519)
- Parafilm (Biozym, cat. no. 743311)
- 12-Well cell culture plate (TPP, cat. no. 92424)
- 60-mm Plastic dishes (Thermo Fisher Scientific, cat. no. 353004)
- Round coverslips (50 mm; VWR, cat. no. 631-0178)
- Round coverslips (18 mm; VWR, cat. no. 631-0153)
- Square coverslips (22 mm; VWR, cat. no. 631-0851)
- Microscope slides (Thermo Fisher Scientific, cat. no. J1800AMNZ)
- Razor blade (Plano, cat. no. T585)
- Silica beads (Sigma-Aldrich, cat. no. 10087)
- Diamond cutter (VWR, cat. no. 201-0392)
- Soft tissue paper (Kimtech Science, cat. no. 7558)
- Lens-cleaning tissues (GE Healthcare, cat. no. 2105-841)
- Pipette Boy (Pipetboy acu 2; Integra Biosciences)
- Vacuum pump (vacuum system; Vacuubrand, cat. no. MZ 2C NT +AK +EK)
- 600-ml Glass beaker (Duran, cat. no. 21 106 48)
- 15-ml Reaction tubes (Corning, cat. no. 352096)
- 50-ml Reaction tubes (Corning, cat. no. 352070)
- 1.5-ml Reaction tubes (Eppendorf, cat. no. 0030120086)
- 10-mm Flexible silicone tubing (VWR, cat. no. 310061010)

- Incubator (VWR, cat. no. INCU-Line IL23)
- Fluorescence microscope: Nikon Ti-Eclipse and Nikon Ti-Eclipse 2 epifluorescence microscopes were used for all images shown here, but our approach can be used with any fluorescence microscope. Setups that offer a semi-automated *z*-stack acquisition and stitching of large images, such as the microscopes used here, are convenient for acquiring large areas for distortion and expansion factor measurements.

Software

- ImageJ (<https://imagej.nih.gov/ij/download.html>) or Fiji (<https://imagej.net/Fiji/Downloads>) in their most up-to-date distribution are recommended, including the BioFormats Importer plug-in bundle (<https://imagej.net/Bio-Formats>). These programs can be used for expansion analysis.
- Python Anaconda can be used for expansion and distortion analysis (<https://www.anaconda.com/download/>). Other programs, such as MATLAB, can be used as well to design custom-written routines but we provide routines for Python Anaconda here.

Reagent setup

PBS

To make PBS, prepare 137 mM NaCl, 2.7 mM KCl, 10 mM Na₂HPO₄, and 2 mM KH₂PO₄ in ddH₂O, and adjust the pH to 7.4. This solution can be stored at room temperature (20–25 °C) for several weeks.

High-salt PBS

To make High-salt PBS, prepare 487 mM NaCl, 2.7 mM KCl, 10 mM Na₂HPO₄, and 2 mM KH₂PO₄ in ddH₂O, and adjust the pH to 7.4. This solution can be stored at room temperature for several weeks.

4% (wt/vol) PFA

To make 4% (wt/vol) PFA, dissolve PFA in PBS to a concentration of 4% (wt/vol). To help the solubilization, stir, heat to 50 °C, and add up to ten drops of 1 M NaOH per 500 ml. The final solution can be stored at –20 °C for at least 6 months.

Extraction buffer

To make extraction buffer, prepare 10 mM MES, 150 mM NaCl, 5 mM EDTA, 5 mM glucose, and 5 mM MgCl₂ in ddH₂O, and adjust the pH to 6.1. After adjusting the pH, add 0.25% (vol/vol) Triton X-100. This solution can be stored at 4 °C for several weeks.

Cytoskeleton buffer

To make cytoskeleton buffer, prepare 10 mM MES, 150 mM NaCl, 5 mM EDTA, 5 mM glucose, and 5 mM MgCl₂ in ddH₂O, and adjust the pH to 6.1. This solution can be stored at 4 °C for several weeks.

Blocking/permeabilization solution

Blocking/permeabilization solution is PBS + 2.5% (wt/vol) BSA + 0.1% (vol/vol) Triton X-100. Prepare the blocking/permeabilization solution fresh each time.

Storage buffer

Storage buffer is PBS + 0.05% (wt/vol) NaN₃. This buffer can be stored at 4 °C for at least 1 month. **! CAUTION** Sodium azide (NaN₃) is acutely toxic, both when ingested as a solid and in solution. Skin contact with the solution can be hazardous as well. Prepare only the amount of solution you require; do not make a concentrated stock and do not store >50 ml of solution containing >0.05% (wt/vol) sodium azide. The solution can be stored at 4 °C for several months.

Anchoring reagent stock

To make anchoring reagent stock, dissolve Acryloyl-X in anhydrous DMSO to a concentration of 10 mg/ml³⁵. Store this stock at –20 °C in a desiccated environment or, if that is not available, in an airtight container with silica beads. An alternative anchoring agent is MA-NHS, which uses the same

chemistry as Acryloyl-X but has a slightly different structure³³. Both anchoring reagents can be stored as described here for at least 3 months.

Anchoring buffer

The anchoring buffer originally proposed and still most widely used^{28,31,33,35} consists of PBS at pH 7.0–7.4. Alternatively, anchoring can be performed in an adjusted version of the anchoring buffer³², resembling a more classic NHS-reaction buffer, consisting of 150 mM NaHCO₃ at pH 8.3 (also see Table 2 for advice on when to apply this optimization). It is usually not necessary to adjust the pH of this solution after dissolving the NaHCO₃; it will usually be pH 8.3 ± 0.2, which is good for use. PBS can be stored at room temperature for several months. The NaHCO₃ buffer should always be prepared fresh and used immediately.

Digestion buffer

The digestion buffer originally proposed and still most widely employed^{28,31,33,35} (consisting of 50 mM TRIS, 800 mM guanidine HCl, 1 mM EDTA, and 0.5% (vol/vol) Triton X-100 in ddH₂O, pH adjusted to 8.0) was adapted from applications of proteinase K in DNA extraction, in which Ca²⁺ is traditionally removed from the solution via EDTA to reduce the activity of DNases present in the sample. However, proteinase K requires Ca²⁺ ions to remain stable and active over prolonged periods of time at high temperatures⁶¹, and DNA preservation is usually not a consideration in protein labeling expansion microscopy. Accordingly, we recommend using an adjusted version of the digestion buffer recipe when performing overnight digestion of mechanically tough samples at 50 °C, to minimize distortions or ruptures³² (also see Table 2 for advice on when to apply this optimization). The improved digestion buffer³² consists of 50 mM TRIS, 800 mM guanidine HCl, 2 mM CaCl₂, and 0.5% (vol/vol) Triton X-100 in ddH₂O, with the pH adjusted to 8.0. Add proteinase K at a concentration of 8 U/ml to either the original or the adjusted digestion buffer directly before use. The buffers can be stored (without proteinase K) at –20 °C for at least 6 months.

Equipment setup

Humidified chamber

Wrap the bottom and lid, separately, of a plastic Petri dish with aluminum foil, and place wet tissues (not dripping) inside the chamber along the circumference.

Gelation chamber

See detailed instructions in Step 17 of the Procedure.

Digestion chamber

Place the sample with digestion buffer into a 12-well plate (or other container with sufficiently big wells to hold the unexpanded gel) and then place the plate on a wet tissue on a sheet of aluminum foil that is large enough to enclose the plate completely. Fold the aluminum foil completely around the plate and close it tightly.

Expansion chamber

Package a plastic Petri dish of appropriate size in aluminum foil to protect the sample from light.

Imaging chamber

Mill out the bottom of a 60-mm plastic Petri dish, leaving a rim of 4–5 mm. Glue in a coverslip with two-component dental silicon. See detailed instructions in Step 26 of the Protocol. **! CAUTION** Beware of mechanical hazards and wear appropriate eye protection when using a milling machine.

Procedure

Immunostaining of 2D cell cultures ● Timing 4–5 h, with 2–3 h of bench time

- 1 Fix the 2D cell culture or primary cells according to a procedure that is appropriate for the cells and proteins of interest. In the example described here, we use cultured hippocampal neurons grown on 18-mm round coverslips.

! CAUTION Many of the common fixatives, including paraformaldehyde and glutaraldehyde, are carcinogens. Methanol is flammable and acutely toxic. Wear appropriate protective equipment and work under a fume hood.

▲ CRITICAL STEP Carry out fixation of cultured cells according to established protocols optimized for each specific protein of interest, whenever such protocols are available (for cultured hippocampal neurons, see, e.g., Glynn and McAllister⁶²; for brain slices, see, e.g., Schneider Gasser et al.⁶³; for cytoskeleton preservation, see, e.g., refs. ^{19,20}). A standard protocol applicable to most proteins uses 4% (wt/vol) PFA in PBS at room temperature for 20–30 min. Standard protocols for cytoskeletal elements (often used for demonstrating expansion microscopy^{28,31,32}) use 100% (wt/wt) methanol for 10–15 min at –20 °C or 0.3% (vol/vol) glutaraldehyde in extraction buffer at 37 °C for 1 min, followed by 10 min in 2% (vol/vol) glutaraldehyde in cytoskeleton buffer at room temperature.

▲ CRITICAL STEP Note that not all commonly used fluorescent dyes are suitable for expansion microscopy. Notably, cyanine dyes are destroyed by the polymerization reaction. The dyes used in this paper are Alexa Fluor 488, Alexa Fluor 546, and CF633; more extensive lists are available in the literature³⁵.

- 2 (Optional) When PFA or glutaraldehyde is used as a fixative, quench its activity before proceeding. Perform quenching of PFA with 1 ml of 100 mM NH₄Cl in PBS at room temperature for 20 min. Perform quenching of glutaraldehyde with 1 ml of freshly prepared 0.1% (wt/vol) borohydride in PBS at room temperature for 7 min, followed by 1 ml of 100 mM NH₄Cl and 100 mM glycine in PBS at room temperature for 10 min. After quenching, wash the samples three times for 5 min each with 1 ml of PBS at room temperature.

▲ CRITICAL STEP Quenching is often omitted in standard immunostainings, but this can degrade the quality of the end result. If quenching is not performed, unreacted groups of PFA and glutaraldehyde remain and can react nonspecifically with antibodies, resulting in unspecific signal. This can lead to unspecific background staining, reducing signal-to-noise ratio during imaging. Optimization of labeling intensity (Steps 4 and 6) is a critical step when preparing samples for expansion microscopy. The most common side effect this can have is increased background. It is therefore particularly important to take steps to decrease background labeling as much as possible.

- 3 Perform blocking and permeabilization in parallel by adding 1 ml of blocking/permeabilization solution, three times for 5 min each, at room temperature.
- 4 Apply the primary antibodies at the concentration suggested by the manufacturer or determined by optimization, in blocking/permeabilization solution, for 1 h, at room temperature, in a humidified chamber. In this example, we use primary antibodies against synaptophysin (1:500 (vol/vol) from a 1 mg/ml stock; guinea pig, Synaptic Systems, cat. no. 101 004), Bassoon (1:100 (vol/vol) from a 1 mg/ml stock; mouse, Enzo, cat. no. SAP7F407), and Homer 1 (1:100 (vol/vol) from a 1 mg/ml stock; rabbit, Synaptic Systems, cat. no. 160 003). To reduce the amount of antibody needed per immunostaining, flip coverslips with cultured cells facing downward onto an 80- μ l droplet of blocking/permeabilization solution with antibody, on a piece of Parafilm inside the humidified chamber.

▲ CRITICAL STEP Fluorescence intensity is often greatly reduced after expansion because of the 3D dilution of dyes per voxel by the cubed expansion factor and other factors (see Introduction, Limitations section, for details). It is therefore essential to optimize antibody concentration and labeling time in order to obtain maximal labeling efficiency during the immunostaining.

- 5 To remove unbound primary antibody from the sample, wash three times with 1 ml of blocking/permeabilization solution each, for 5 min each, at room temperature.
- 6 Apply the secondary antibodies at the concentration suggested by the manufacturer or determined by optimization, in blocking/permeabilization solution, for 1 h, at room temperature, in a humidified chamber. In the experiments presented here, we use secondary antibodies against guinea pig IgG (conjugated to Alexa Fluor 488; Dianova, cat. no. 706-545-148), mouse IgG (conjugated to CF633; Biotium, cat. no. 20124), and rabbit IgG (conjugated to Alexa Fluor 546; Thermo Fisher Scientific, cat. no. A-11035); all antibodies were used at 1:100 (vol/vol) antibody stock to blocking/permeabilization solution ratio from a 0.6-mg/ml stock. To reduce the amount of antibody needed per immunostaining, coverslips with cultured cells can be flipped with the cells facing downward onto an 80- μ l droplet of blocking/permeabilization solution with antibody on a piece of Parafilm inside the humidified chamber.

▲ CRITICAL STEP Although it is possible to further increase labeling by increasing the concentration or incubation time (such as in Step 4) of the secondary antibody, this also carries an increased risk of unspecific binding. We therefore recommend beginning optimization of labeling efficiency with the primary antibody incubation.

- 7 To remove unbound secondary antibody from the sample, wash it three times with 1 ml of blocking/permeabilization solution, for 5 min each, at room temperature. Then wash it two times with PBS to remove the BSA and Triton X-100 contained in the blocking/permeabilization solution from the sample.
■ PAUSE POINT Samples immunostained as described here can be stored in storage buffer at 4 °C for up to 4 weeks. Protect the samples from light to avoid bleaching.
- 8 Acquire an overview image of the sample if you are planning to use the method described in Step 31C for determining the expansion factor. This is highly recommended (see Step 31 and Fig. 7 for details). Alternatively, determine the weight or the diameter of the gel when following Step 31A or B, respectively.

Anchoring ● Timing >6 h, overnight

- 9 Thaw the stock of the anchoring reagent, Acryloyl-X³⁵ or MA-NHS³³ (see Reagent setup). Acryloyl-X and MA-NHS use the same chemistry for anchoring and gel integration, and have only slightly different structures. MA-NHS can therefore be used as an alternative anchoring reagent equivalent to Acryloyl-X, as described previously³³.
▲ CRITICAL STEP Acryloyl-X and MA-NHS lose reactivity after prolonged storage, especially when coming into contact with water. It is therefore imperative to maintain the stocks in a desiccated environment.
- 10 Dilute Acryloyl-X 1:100 (vol/vol) to 0.1 mg/ml in anchoring buffer (see also Fig. 2). Perform anchoring by placing an 80-μl droplet of the anchoring solution onto a piece of Parafilm in a humidified chamber, and flipping the coverslip onto it with the cells facing down. Incubate the sample with the anchoring solution for at least 6 h or overnight (depending on the sample, it may be possible to reduce this to 2–3 h⁴⁰).
▲ CRITICAL STEP Anchoring is essential for integrating the sample into the gel matrix later on. If anchoring is insufficient, the fluorophores applied during the immunostaining will not be fixed in their relative positions, resulting in loss of fluorophores. In addition, insufficient anchoring results in distortions or ruptures of the sample during expansion (Fig. 2c). This can be avoided by using the adjusted anchoring buffer described in the Reagent setup (also see Table 2 for when to apply this optimization).
- 11 Wash the sample two times in 1 ml of PBS, 5 min each, at room temperature, right before application of the gelation solution (see the next section, Polymerization).

Polymerization of X10 gel ● Timing >2 h

- 12 Mix the gel monomer components as given in the table below (amounts are given as an example for 5 ml of polymerization solution; the remaining 0.5 ml of volume is reserved for KPS solution to be added in Step 15) in a 50-ml reaction tube:

Chemical	Mol%	Weight (g)
DMAA	80	1.335
Sodium acrylate	20	0.32
ddH ₂ O	Not applicable	2.850

Vortex the solution well to dissolve the sodium acrylate. The final solution will be slightly turbid, but no grains should remain.

! CAUTION *N,N*-dimethylacrylamide (DMAA) is corrosive and acutely toxic. Sodium acrylate is dangerous to the aquatic environment. Wear appropriate protective equipment and work under a fume hood.

▲ CRITICAL STEP It is important to maintain the exact molar ratio of DMAA to sodium acrylate (80:20) here to reach the expected expansion factor of tenfold. Increasing the concentration of DMAA relative to SA will reduce the expansion factor, whereas decreasing the concentration of DMAA relative to sodium acrylate beyond the 80:20 ratio will not substantially increase the expansion factor any further, but will result in a less stable gel. We strongly recommend weighing all components, including the ddH₂O. The volume of prepared gel can be reduced for the number of samples used (80 μl is sufficient for one 18-mm coverslip). However, we strongly recommend not reducing the volume too much, as measuring errors in this step and in Step 15 can increase fluctuations in the expansion factor from

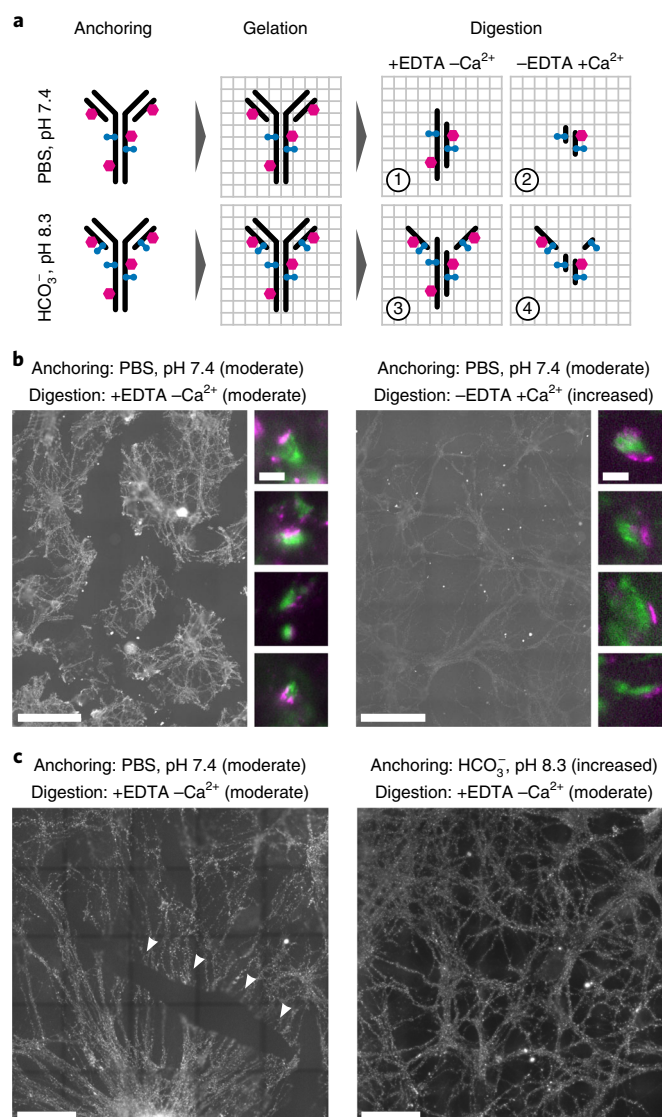


Fig. 2 | Anchoring and homogenization conditions can be optimized for the specific requirements of the sample and experiment. a, Optimizations for anchoring and homogenization and the trade-offs that may come with them. The black drawings represents antibodies, the magenta hexagons represent fluorophores, the blue handles represent the anchoring reagent, and the gray grid represents the expansion gel. In conditions 1 and 2, anchoring is performed in PBS at pH 7.4, whereas in conditions 3 and 4, anchoring is performed in HCO_3^- at pH 8.3. In conditions 2 and 4, proteolytic homogenization with proteinase K is performed in the presence of Ca^{2+} . The presence of calcium leads to higher digestion, whereas the use of HCO_3^- leads to higher anchoring. **b**, Effect of increased digestion on mechanical homogenization and fluorophore retention. These exemplary X10 microscopy images show immunostainings in primary hippocampal cultures for synaptophysin (grayscale in the overviews, green in the magnifications) and the postsynaptic protein Homer 1 (magenta, only in the magnifications). Both samples were immunostained, expanded, and imaged in parallel under identical experimental conditions in the overview images, except for the digestion buffer. Anchoring was moderate in PBS at pH 7.4. The moderate digestion condition (left) corresponds to condition 1 in **a**, and the intense homogenization condition (right) corresponds to condition 2 in **a**. Expansion factors: left, 10.3 \times ; right, 10.5 \times . Scale bars, overviews, 100 μm ; magnifications, 500 nm. **c**, Effect of anchoring on sample stability. Exemplary X10 images of hippocampal neuron cultures immunostained for the synaptic vesicle protein synaptophysin, visualizing synapses, with two different conditions for anchoring. The moderate anchoring condition (left; arrowheads: ruptures) corresponds to condition 1 in **a**, and the increased anchoring condition (right; no ruptures) corresponds to condition 3 in **a**. Expansion factors: left, 9.1 \times ; right, 9.0 \times . Scale bars, 50 μm . Images were taken on a wide-field microscope.

experiment to experiment. The reason for this is that the X10 gel varies in the attainable expansion factor depending on the exact molar ratios of DMAA and sodium acrylate. Also, purging of oxygen (Step 13) with N_2 or argon gas is usually easier in sufficiently large volumes. Experience has shown that the 5-ml volume given here is a volume for which errors are usually small and results are robust.

- 13 Purge O₂ from the monomer solution by bubbling with N₂ or argon gas for at least 40 min, at room temperature. If there is no N₂ or argon gas available in your lab, evaporate liquid nitrogen in a plastic bottle with a tube connected to it. To regulate the gas flow, place the plastic bottle in a liquid nitrogen transport container with a variable amount of liquid nitrogen around it or apply an adjustable nozzle to the outlet tube. In the meantime, proceed with Step 14.
▲ CRITICAL STEP This step is essential to ensure gelation. Molecular oxygen inhibits the polymerization reaction of DMAA and sodium acrylate, and thus needs to be purged from the gelation solution completely. The polymerization reaction of the classic fourfold expanding gel²⁸ has now been suggested⁴⁰ to also profit from the purging of O₂. Ideally, use the solution immediately after purging to ensure that oxygen is not reintroduced through contact with the atmosphere.
- 14 Prepare a 0.036 g/ml stock of KPS in ddH₂O while the monomer solution is purging. Add the ddH₂O immediately before you want to use the solution in Step 15. Dissolving KPS at this concentration usually requires vigorous vortexing for 1–2 min.
▲ CRITICAL STEP KPS is unstable in aqueous solution and rapidly loses reactivity. Storing the stock, or even preparing it too far in advance of using it, is therefore not advised. Always prepare the stock fresh, and discard unused stock solution.
- 15 After purging is complete, transfer 2.7 ml from the 50-ml reaction tube used in Step 13 to a fresh 15-ml reaction tube. Add 0.4 mol% KPS relative to the monomer concentration by adding 0.3 ml of the stock prepared in Step 14 to the 2.7 ml of the monomer solution. This will yield 3 ml of gelation solution. To prevent premature polymerization, prepare the monomer solution first in the fresh 15-ml reaction tube, then add KPS stock, quickly vortex for 1–3 s, and immediately proceed to Step 16. Again, the volumes can be adjusted as needed, but it is recommended to avoid reducing them too much, to avoid measurement errors and to make purging with N₂ or argon gas easier.
▲ CRITICAL STEP It is imperative to precisely maintain the molar ratios of monomers to KPS to ensure proper polymerization, so careful measurements of the volumes of KPS stock and monomer solutions used here are essential.
- 16 Purge the polymerization solution prepared in Step 15 of O₂ again by bubbling with N₂ or argon gas for 15 min on ice. In the meantime, proceed with Step 17.
▲ CRITICAL STEP It is imperative to bring the gelation solution to 0 °C for this step, as the addition of KPS will otherwise initiate premature polymerization. To facilitate a quick heat exchange, place the reaction tube with the polymerization solution into a large container (>0.5–1 liter) filled with crushed ice and cold water. It is usually not sufficient to use crushed ice without water, as the air pockets between the crushed ice are insulating and prevent a quick heat exchange (i.e., the gelation solution will be considerably warmer than 0 °C and polymerization can occur prematurely).
? TROUBLESHOOTING
- 17 Prepare gelation chambers for your samples (Fig. 3) while the polymerization solution is purging. To build a gelation chamber, label a microscopy slide and use a diamond knife to cut a square 22 × 22-mm coverslip into four strips of roughly equal width (Fig. 3b, panel 1). Place two of the strips on the microscopy slide, leaving space between them for the coverslip with the labeled and anchored sample (Fig. 3b, panel 2). To stick the coverslip strips to the microscopy slide, apply a small volume (<1 µl) of water or PBS from the side, and let it get sucked below the strip. The strip will stick to the coverslip now but can still be moved easily with forceps to adjust the distance between the strips for the sample. Place the coverslip with the sample facing up onto the microscopy slide between the two strips (Fig. 3b, panel 3). Carefully remove the liquid from the coverslip as completely as possible, as remnants of the solutions used for anchoring or washing can dilute the gelation solution applied later, resulting in incomplete polymerization. It is often helpful to air-dry the sample briefly in addition. Place the other two strips of coverslip such that they overlap the coverslip with sample and the two flanking strips of coverslip (Fig. 3b, panel 4). Place a whole 22 × 22-mm coverslip on top of the sample, using the coverslip strips placed before as pedestals (Fig. 3b, panel 5). To ease application of the gelation solution, shift the top coverslip so that part of the sample remains exposed (top edge in the schematic).
▲ CRITICAL STEP The timing of this step with respect to Steps 18 and 19 is important. Do not leave the coverslips with the cell culture sample long enough for the sample to completely dry out before finalization of the polymerization solution in Step 18 and its application to the sample in Step 19. A brief air-drying to remove residual moisture adhering to the coverslip can nonetheless improve the outcome.
- 18 Remove 500 µl of polymerization solution, prepared in Step 16, and transfer it to a fresh 1.5-ml reaction tube. Add 2 µl of TEMED (100% (wt/wt)) to the 500 µl of polymerization solution (or an

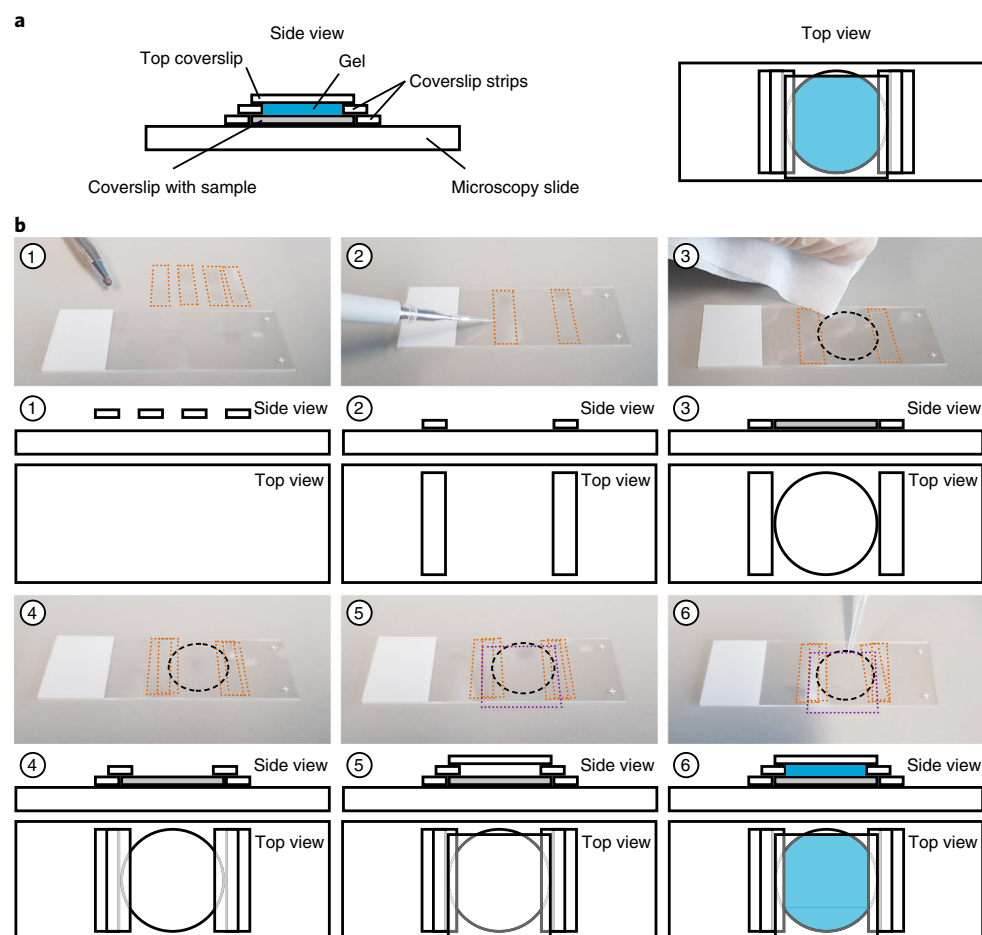


Fig. 3 | Assembly of a gelation chamber (Step 17). **a**, Schematic showing the assembled gelation chamber in side view (left) and top view (right). **b**, Step-by-step assembly of the gelation chamber with photographs (top) and the corresponding schematics (bottom): (1) cut a 22 × 22-mm glass coverslip into four strips, (2) place two of those strips on the microscopy slide and immobilize them with a drop of water or PBS, (3) place the coverslip with the sample between the strips, (4) place the two remaining strips on top of the place where the first two strips and the sample coverslip meet, (5) place a 22 × 22-mm coverslip on top, and (6) add the gelation solution from the side (see Steps 17 and 19 for details). For better visibility, glass coverslips are additionally traced out in the photographs. The coverslip containing the sample is indicated with a dashed black outline. The coverslip strips used to hold up the top coverslip of the chamber are indicated with dotted orange outlines. The top coverslip used to close the chamber is indicated with a dotted purple outline.

adjusted amount, if you choose to change the volume). Vortex briefly for 1–3 s and immediately proceed to Step 19.

▲ CRITICAL STEP Initial polymerization after addition of TEMED is extremely rapid, so adding the gel to the sample quickly is essential (ideally within seconds and well <1 min). Keep the polymerization solution on ice (again with water) after addition of TEMED to delay polymerization, but note that rapid work is still essential in this step. Monitor whether polymerization was successful by keeping a small amount (100–200 μ l) of polymerization solution + TEMED in a reaction tube at room temperature. After ~5–10 min, the solution will start to harden and become noticeably warm to the touch.

? TROUBLESHOOTING

- 19 Apply the polymerization solution with TEMED to the sample in the gelation chamber (50–60 μ l per 18-mm-diameter coverslip), pipetting from the open end of the assembly (Fig. 3b, panel 6).

▲ CRITICAL STEP It is essential to work quickly here. After addition of TEMED, bring the gelation solution into contact with the sample, ideally within seconds and certainly before 1 min has passed. As the initial stage of polymerization is proceeding rapidly, this is essential to ensure integration of Acryloyl-X into the growing gel meshwork.

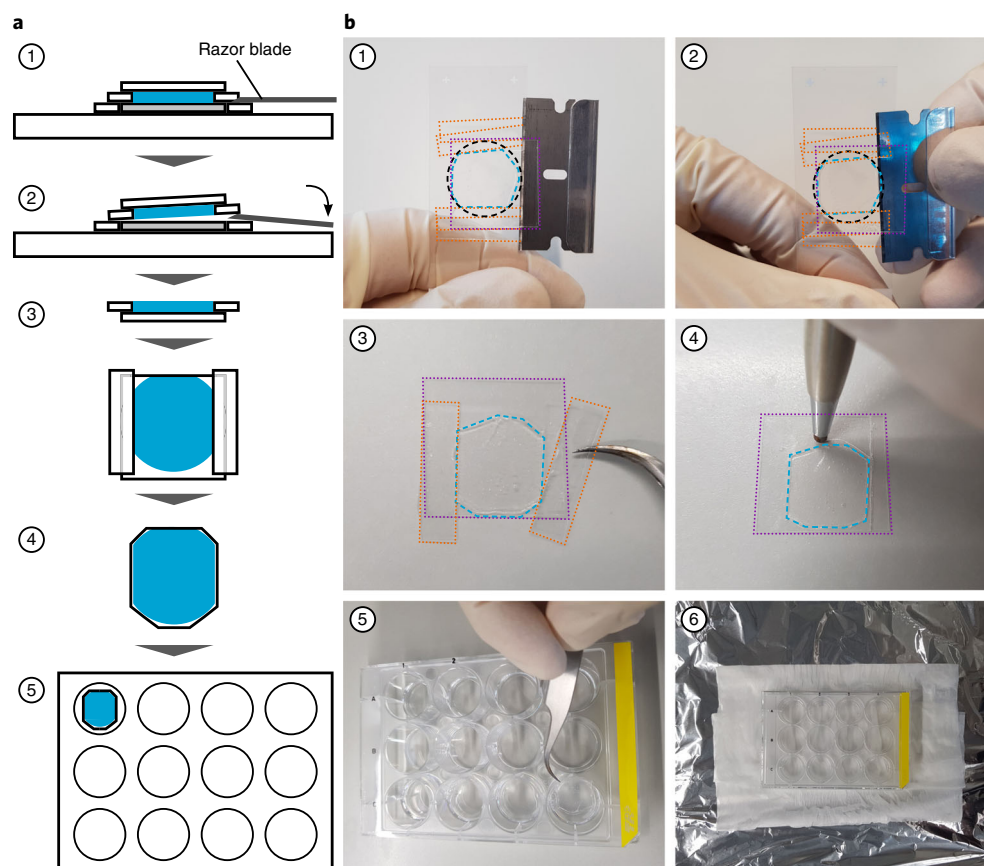


Fig. 4 | Removal of the gel from the gelation chamber and assembly of a digestion chamber (Step 22). **a**, Schematic showing how to remove the polymerized gel from the gelation chamber and how to place it into a digestion chamber. **b**, Illustration of the process with photographs in which glass coverslips and the gel are additionally outlined for better visibility: (1) insert a razor blade under the top 22 × 22-mm coverslip, (2) gently press the razor blade upward and lift off the top coverslip with the polymerized gel sticking to it, (3) lay out the top coverslip on a work surface with the polymerized gel facing up and use forceps to remove the glass coverslip strips sticking to it, (4) use a diamond cutter to trim the top coverslip around the polymerized gel, (5) place the trimmed top coverslip with the polymerized gel facing up in a prepared digestion chamber, and (6) package the digestion chamber in aluminum foil with wet tissues (see Step 22 for details). The coverslip containing the sample is indicated with a dashed black outline. The coverslip strips used to hold up the top coverslip of the chamber are indicated with dotted orange outlines. The polymerized gel is indicated with a dashed blue outline. The top coverslip, used to close the chamber, is indicated with a dotted purple outline. See Step 22 of the Procedure for further explanation.

20 Let the gel polymerize by incubating for 1 h in a humidified chamber, at room temperature.

▲ CRITICAL STEP The polymerization should be completed after 1 h, but it is useful to test the consistency of the gel before proceeding. To do this, gently try to lift the coverslip closing the gelation chamber on the top upward with forceps from below. The coverslip should not detach easily or slide on the gel.

? TROUBLESHOOTING

■ PAUSE POINT After polymerization, the sample can be stored in a humidified chamber (take care that it remains humidified for the entire storage time to avoid drying) and protected from light (to avoid bleaching) at room temperature for up to 1 week before proceeding.

Homogenization ● Timing >12 h, overnight

21 Thaw the digestion buffer and add proteinase K to a dilution of ~8 U/ml. For each 18-mm coverslip with sample, add 1 ml of digestion buffer to an individual well of a 12-well plate.

▲ CRITICAL STEP Homogenization of the sample by digestion is essential to reduce resistance during expansion. If this is not performed sufficiently, the sample can tear (Fig. 2).

22 Remove the gel from the gelation chamber to transfer it to the digestion solution (Fig. 4). To remove the gel from the gelation chamber, insert a razor blade between the two stacked coverslip

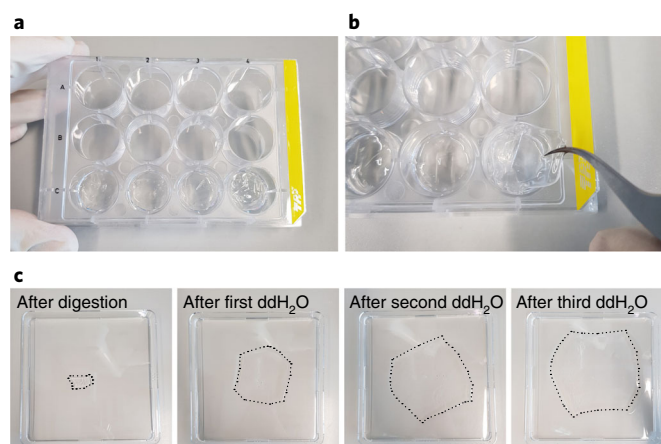


Fig. 5 | Expansion of the homogenized sample (Steps 24 and 25). **a**, The sample gel appears swollen after digestion, giving it a ruffled appearance and drawing in some of the digestion buffer. This is normal and no cause for concern. **b**, Forceps are used to remove the sample from the 12-well plate. See Step 24 of the Procedure for further explanation. **c**, Gel expansion during three steps of ddH₂O exchange. Because the gels have low contrast, they are outlined by black dotted lines here for better visibility. For scale, the edge length of the expansion chamber is 24.5 cm. See Step 25 of the Procedure for further explanation.

strips used as pedestals to hold up the top 22 × 22-mm coverslip. The flat side of the blade should be pointing down (Fig. 4a,b, panel 1). Carefully lift the top coverslip off by gently applying downward pressure onto the razor blade (Fig. 4a,b, panel 2). The gel will usually detach from the sample coverslip and stick to the top coverslip. This is not an issue, as the sample is covalently integrated into the gel by anchoring after polymerization. If the gel sticks to the sides of the coverslip strips at the edges, use another razor blade to cut it loose carefully. Place the top coverslip with the gel on a benchtop work surface, with the gel facing up, and carefully remove the coverslip strips that were used as pedestals (Fig. 4a,b, panel 3). Use a diamond cutter to trim away the parts of the 22 × 22-mm coverslip that do not contain gel, to make it fit into a well of a 12-well plate (Fig. 4a,b, panel 4). Place the trimmed coverslip into a well of a 12-well plate containing digestion buffer with proteinase K, with the gel facing up (Fig. 4a,b, panel 5). Do not use the middle row, as removing the samples after digestion will be much easier when they can be spooned out from one of the outer wells (Step 24). Place the 12-well plate onto a sheet of aluminum foil with wet tissues, package it well by folding the foil, and place it into an incubator for digestion (Fig. 4b, panel 6).

? TROUBLESHOOTING

- 23 Incubate each sample in digestion buffer with proteinase K for >8 h, or overnight in a humidified digestion chamber, at 50 °C.

▲ CRITICAL STEP Digestion is highly dependent on temperature, digestion time, pH, composition of the digestion buffer, and enzyme quality. When working with the lower expansion factor of the classic 4× gel, for which less homogenization is sufficient to avoid tears, the digestion time can be reduced to 2 h^{28,40} for samples that are mechanically less tough, e.g., 2D cell cultures. Proteinase K has its activity optimum at 50–55 °C, tolerates a wide range of pH values (8.0–12.0) without noticeable alteration of activity, and requires Ca²⁺ for maintaining activity over prolonged periods of time. To obtain optimum results in terms of structural preservation, heat the sample and use the adjusted digestion buffer described here (see Reagent setup, ‘Digestion buffer’). However, note that with current anchoring technology, there is an inherent trade-off between the degree of homogenization and retention of fluorophores. Hence, the increased activity of proteinase K in the adjusted digestion buffer can lead to signal loss if anchoring is insufficient (Fig. 2; also see additional instructions in the Reagent setup and Table 2).

Expansion ● Timing 1–2 h

- 24 Remove the gel from the digestion chamber by using forceps to grip it together with the coverslip it came on (Fig. 5). If polymerization was successful, the gel is stable enough for lifting it out of the well in this way (Fig. 5b). Place the coverslip with the gel directly into an expansion chamber that is large enough to hold the final anticipated gel volume (e.g., a 245-mm square plastic tray; Fig. 5c). If

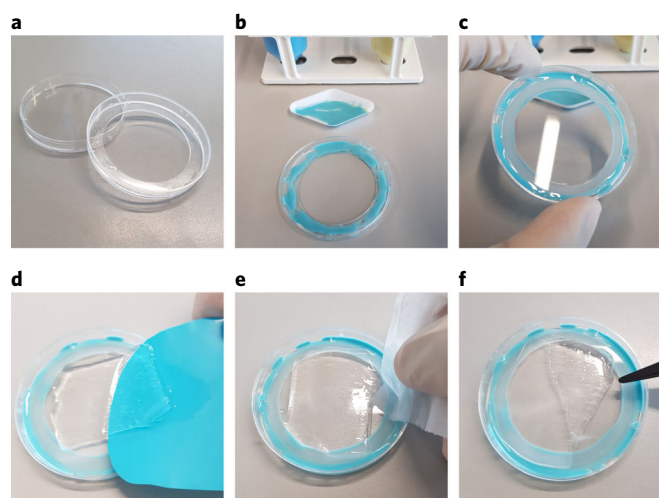


Fig. 6 | Assembly of an imaging chamber (Steps 26 and 27). **a**, A 60-mm plastic dish from which the bottom has been removed, e.g., by cutting it out with a milling machine at a professional workshop. Leave a rim of 4–5 mm. **b**, A two-component dental silicone is mixed 1:1 (vol/vol) and distributed as a thin film on the inside of the remaining rim. **c**, A 50-mm coverslip of thickness appropriate for the microscope objectives to be used for imaging (typically no. 1 or no. 1.5) is pressed into the silicone. **d**, A thin piece of plastic, e.g., the cut-out bottom of a weighing pan, is used to separate the gel into pieces that are small enough to fit into the imaging chamber. **e**, Excess water is removed from the gel by dabbing the edges with a tissue. This reduces sample drift during imaging. **f**, Another 50-mm coverslip is placed on top of the gel to stabilize it; it is now ready for imaging.

this is difficult to achieve, the gel can alternatively be removed by inserting a plastic or metal spatula below the gel and spooning it out with one gentle but swift motion. Add an excess of ddH₂O exceeding ten times the expected final gel volume (300–500 ml is typically ideal for a sample that started on an 18-mm coverslip).

▲ CRITICAL STEP It is important to work carefully and not to tear the gel here. Gripping the gel with forceps can require some practice, but usually does not damage the sample if done carefully (see Fig. 5 for details). Alternatively, use a plastic or metal spatula for gently spooning the gel out of the 12-well plate and into the expansion chamber. If the gel does not immediately unfold or is partially wrapped around the coverslip (see first image in Fig. 5c, after digestion), do not attempt to unfurl it; this will occur naturally during expansion, with much less chance of damaging the gel.

? TROUBLESHOOTING

- 25 Remove the ddH₂O after 10–20 min of incubation, using a Pipetboy or a vacuum pump. Add fresh ddH₂O. Repeat this step until no further expansion of the gel can be observed (usually after three to four water exchanges; Fig. 5c).

▲ CRITICAL STEP It is important to work carefully and not to aspirate the gel here.

? TROUBLESHOOTING

■ PAUSE POINT Expanded samples can be stored for up to 1 month at 20–25 or 4 °C. Replace any evaporated water to avoid drying and protect the sample from light to avoid bleaching during storage. For optimal results, samples should be imaged as soon as possible after preparation, to avoid degradation of fluorophores.

Imaging ● Timing variable

- 26 Assemble an imaging chamber by milling out the bottom of a 60-mm plastic Petri dish, but leave a rim of 4–5 mm (Fig. 6). Next, mix two-component dental silicon and apply a layer to the rim that is left. Immediately push a 50-mm coverslip into the glue and let it harden for a few minutes. The coverslip should be matched to the objectives intended for imaging (typically, no. 1.5 for oil objectives; see the advice in the Troubleshooting section for Step 30 for further details), as this is the coverslip through which the sample will be imaged. Remove any excess glue with a razor blade or scalpel.

! CAUTION Beware of mechanical hazards and wear appropriate eye protection when using a milling machine.

- 27 Remove all ddH₂O from the completely expanded sample with a Pipetboy or vacuum pump and paper tissues, and use a thin plastic piece (e.g., the cutout bottom of a weighing pan) to cut the gel

into small pieces that fit into the imaging chamber. Transfer one piece to an imaging chamber and place another 50-mm coverslip on top.

- 28 Place the imaging chamber into the microscope you wish to use for imaging, ideally an inverted setup, and begin imaging by locating the sample focus.

? TROUBLESHOOTING

- 29 Take an overview image with a low-magnification objective if you would like to use the recommended method (described in Step 31C) for determining the expansion factor and distortions of the sample.

▲ CRITICAL STEP It is ideal to do this with a semi-automated microscope stage. A slide scanner can be useful as well.

? TROUBLESHOOTING

- 30 Proceed with imaging your sample until all data you wish to acquire are collected. To maximize imaging outcome, it is important to keep in mind all factors that determine image quality, e.g., selection of high-numerical-aperture objectives, matching of the coverslip thickness to the objective used, and matching of the refractive index of the objective immersion medium to that of the sample to avoid spherical aberrations and achieve higher imaging depth.

? TROUBLESHOOTING

Validation ● Timing variable

- 31 To determine the expansion factor, three methods have been used in the past. Follow option A to determine the expansion factor based on the increase in weight of the gel. Follow option B to determine the expansion factor by measuring the increase in diameter of the gel. Follow option C for a microscopy-based analysis of the expansion factor. In our experience, option C is the most reliable method and is highly recommended for good practice.

▲ CRITICAL Determining the expansion factor is essential for being able to provide an accurate scale bar for expansion microscopy images and for giving accurate numbers for distance measurements. The expansion factor should be determined for each sample individually, because the precise expansion factor varies from sample to sample.

(A) Determination of the expansion factor by weight

▲ CRITICAL This method is usually imprecise because it is difficult to remove all excess water adhering to the gel, usually resulting in an overestimation of the expansion factor.

(i) Weigh the gel after expansion.

- (ii) Calculate the ratio of the expanded weight to the original weight, as determined in Step 8. The obtained ratio is equal to the 3D expansion factor (volumetric expansion factor)³⁹. To obtain the linear expansion factor, calculate the third root of the volumetric expansion factor.

(B) Determination of the expansion factor by diameter

▲ CRITICAL This method is usually imprecise because gels are rarely completely symmetrical, and small differences in the axis on which the diameter is measured before and after expansion can lead to large errors. Furthermore, because there is insufficient contrast between the gel and adhering water after expansion, it is difficult to measure with sufficient precision, resulting in under- or overestimations of the expansion factor.

(i) Measure the diameter of the gel after expansion.

- (ii) Calculate the ratio of the expanded diameter over the original diameter, as determined in Step 8. The obtained ratio is equal to the expansion factor³⁹.

(C) Determination of the expansion factor by microscopy analysis

▲ CRITICAL This is the method originally suggested by the Boyden lab²⁸, and it should be considered the gold standard (Fig. 7). This method is more time consuming than the previously mentioned ones, yet it is highly recommended for its precision, as it measures the physical expansion directly on the sample itself.

(i) Acquire another overview microscope image after expansion. Expect that imaging parameters must be adjusted to obtain similar brightness to that in Step 8.

- (ii) Match the same structures and determine their relative sizes. Ideally, these images should be stitched from several frames at low magnification in the brightest and highest-contrast imaging channel available for the sample. The goal is to obtain images in which the organization of the sample is clearly visible and to make sure that the same structures are revisited that were imaged before expansion in Step 8.

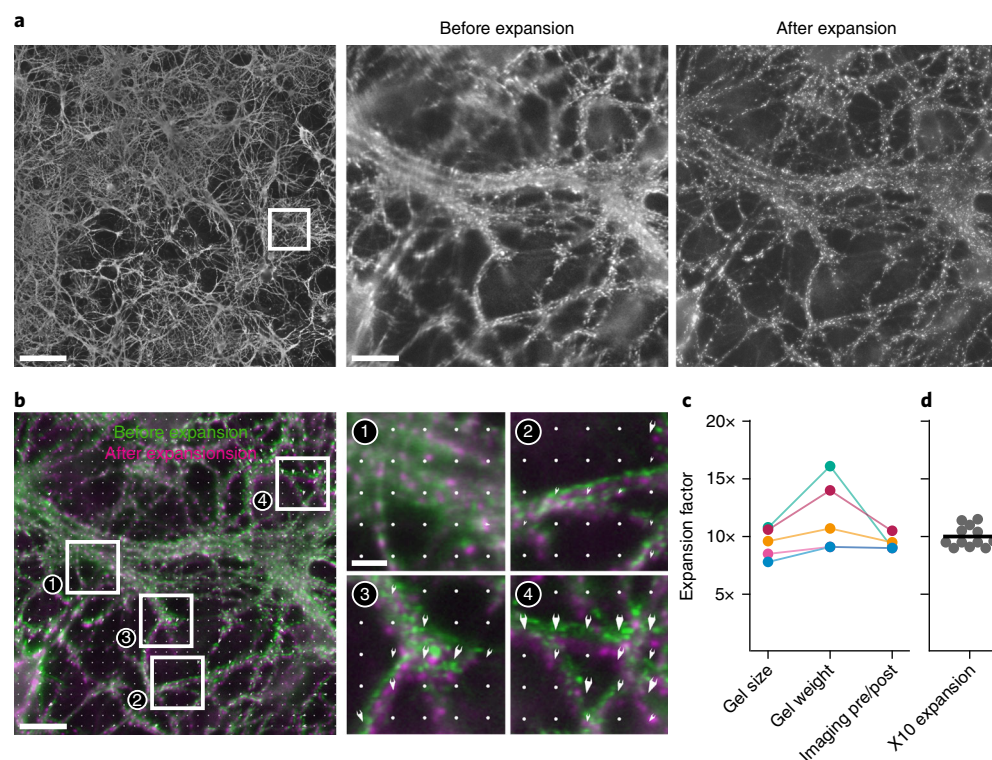


Fig. 7 | Exemplary images of samples before and after expansion, and quantification of expansion factor and distortions. **a**, Exemplary images showing overviews of primary hippocampal neuron cultures stained for synaptophysin, a synaptic vesicle protein, allowing visualization of synapses. The white box in the left-hand image is magnified in the middle and right images. The overview image on the left and the first magnified image were taken before expansion; the second magnified image was taken after expansion. Expansion factor: 8.0 \times . Scale bars, overview, 200 μ m; magnified views, 20 μ m. **b**, Overlay of the images from **a** (before expansion, green; after expansion, magenta). This overlay was automatically generated using the Python scripts from Supplementary Data 1. The vector map overlaid as white arrows indicates local distortions, for which arrow length indicates the magnitude of local offset between pre- and post-expansion images. The boxed regions are magnified to show areas of small and larger shifts. Scale bars, overview, 20 μ m; magnifications, 5 μ m. **c**, Expansion factors measured on five different samples (individual samples color-coded and connected by lines), using three different techniques in parallel: determination of the expansion factor by weight (gel weight, option A in Step 31), determination of the expansion factor by diameter (gel size; option B in Step 31), and determination of the expansion factor by microscopy analysis (imaging pre- and post-expansion, option C in Step 31). On average, the expansion factor predicted by measuring the gel size is off by ~6% in the data quantified here, whereas the expansion factor predicted by measuring the gel weight is off by ~18% in the data quantified here. **d**, Typical spread of expansion factors to be expected from X10 experiments, quantified by comparing pre- and post-expansion images of the same sample directly (mean \pm s.e.m., 10.0 \pm 0.27; n = 12 independent experiments).

- (iii) Overlay the pre- and the post-expansion images by shifting, rotating, and scaling to find the alignment where they correspond best.

? TROUBLESHOOTING

- (iv) Using the distance measurement tool in ImageJ (Supplementary Fig. 1) or custom-written Python routines (Fig. 7), measure the distance of clearly identifiable landmarks.

▲ CRITICAL STEP The Python script we provide with this paper (Supplementary Data 1) should dramatically reduce the time requirements of this step. Included with the script are a readme file explaining installation and application, and sample data to test it on (the same data shown in Fig. 7 and Supplementary Fig. 1). The script is written and tested for Windows 10 as an operating platform, but it is also useable on other platforms because of the wide compatibility of Python 3.6. However, samples differ in organization and quality, which may cause problems in successful pattern recognition for the script. In such cases, the manual or a semiautomatic approach may remain necessary.

- (v) When using the manual approach, measure at least ten such distances, calculate the average, and use it as the determined expansion factor (Supplementary Fig. 1).

- (vi) Once the expansion factor is determined, convert the physical pixel size of the images taken to the effective pixel size by simply dividing the physical pixel size by the expansion factor. Scale down scale bars and distance measurements accordingly by dividing by the expansion factor.
- 32 To determine distortions, overlay the same pre- and post-expansion images used for determining the expansion factor in Step 31C (Fig. 7). To evaluate distortions on a finer scale, dedicated comparison images acquired with high numerical aperture (NA) objectives are preferable. To measure distortions, overlay the pre- and post-expansion images, using (a) custom-written Python routines or other scripts or (b) manual alignment, and analyze them with custom-written Python routines or other scripts. Our Python script is available as Supplementary Data 1; this includes a readme file explaining installation and use of the script, the script itself, and sample data on which to test the script (the same data as shown in Fig. 7 and Supplementary Fig. 1).

▲ CRITICAL STEP A general caveat for distortion measurements is that the pre-expansion images are diffraction limited, whereas the post-expansion images are super-resolution images. This means that nanoscale distortions can usually not be determined, for lack of resolution on the pre-expanded images. This problem can be addressed by comparison with other super-resolution techniques. This has in the past resulted in observations that closely match between expansion microscopy and other super-resolution methods^{28,31–33,35}, which supports the notion that nanoscale architecture is also preserved. If the pertinent equipment and expertise are available, it is possible to consider evaluating nanoscale distortions for a particular type of sample by comparing post-expansion images with pre-expansion super-resolution images of the same structure. Because the idiosyncrasies of the different expansion microscopy techniques can produce images of vastly different resolution, organization, and overall quality, universally applicable guidelines are difficult to provide, and it might be necessary to adapt the scripts used for distortion measurements.

▲ CRITICAL STEP Evaluating the distortions is not necessarily useful for every single sample. Although local distortions can vary from sample to sample, as well as within the same sample, overall magnitudes and patterns in the vector fields describing distortions from the same type of sample will usually be very similar^{28,31,32}. However, distortion analysis should nonetheless be performed routinely, even on the same type of sample, to ensure that the obtained data are of uniform quality and the results are trustworthy. Between different types of samples, distortions can be more variable, especially when the mechanical properties of the samples differ. When using the additional distortion analysis Python script provided with this paper (Supplementary Data 1), performing distortion analyses as a regular part of the analysis of each sample is trivial. We recommend performing distortion analyses routinely in parallel to expansion factor calculation.

? TROUBLESHOOTING

Troubleshooting

Troubleshooting advice can be found in Table 3.

Table 3 | Troubleshooting table

Step	Problem	Possible reason	Solution
16	The gel polymerizes or partially gels during the second O ₂ purging step, after addition of KPS	KPS probably prematurely initiated the polymerization reaction during the second O ₂ purging	The second purging step is included to remove O ₂ from the KPS stock that has been added. To avoid the second purging step (of monomer solution + KPS), adding KPS as a solid is possible. However, the small amount necessary usually introduces unacceptable weighing errors. Alternatively, purge the KPS solution of O ₂ separately before adding it to the monomer solution, and use the resulting polymerization solution immediately, without a second purging step. However, this necessitates the preparation of KPS in parallel with the monomer solution, which also means that it has more time to degrade (Step 14). Generally, the better solution is to ensure that the polymerization solution is maintained at 0 °C, as described in Step 16. This can be monitored with a noncontact thermometer if necessary
18	The entire polymerization solution + TEMED polymerized or partially gelled before it could be added to the sample	The polymerization reaction proceeded too quickly	The polymerization reaction is difficult to delay efficiently. It is often useful to use only a small amount of gelation solution during this step (e.g., 500 µl of gelation solution + 2 µl of TEMED) and keep the rest bubbling with N ₂ at 0 °C for later use. Polymerization is initialized extremely quickly upon addition of TEMED, and the gelation solution should thus be brought into contact with the sample as quickly as possible after addition of TEMED, so working in small portions is usually desirable (especially if working with many samples in parallel). In addition, keep the polymerization solution at 0 °C after adding TEMED

Table continued

Table 3 (continued)

Step	Problem	Possible reason	Solution
20	The gel does not polymerize or gels only partially	The sodium acrylate may be of insufficient quality (Step 12)	Store sodium acrylate desiccated at -20°C for up to 3 months to prevent decomposition through reaction with atmospheric water. Close the lid with Parafilm and wipe it before opening and closing, to reduce exposure to moisture from condensation when warming the sodium acrylate to room temperature. To check purity, make a stock (38 g per 100 ml); the stock should be almost completely transparent; if the stock has a noticeable yellow tint, discard the sodium acrylate batch and open a new one. Check this upon first opening a new batch, and repeat the check regularly (at least once a month) until the batch is used up
		The purging of O_2 may have been incomplete (Step 13)	Monitor the amount of bubbling in the solution. There should be a constant flow, but no substantial squirting of solution to the walls of or out of the reaction tube. It is generally not necessary to actually monitor the O_2 content, as the 40-min time for purging was chosen with a large safety margin
		The ratio of KPS to monomers may have been incorrect (Step 15)	As some of the monomer solution often splashes against the walls of the container during bubbling, precision is improved by transferring a defined amount of monomer solution to a new container before adding the appropriate amount of KPS (e.g., 2.7 ml of monomer solution + 0.3 ml of 0.036 g/ml KPS stock). This will ensure that the molar ratios of monomers and KPS are precisely as intended, which is critical to ensuring polymerization. To ensure that all of the solution is purged equally, check regularly (every 5–10 min) during purging if splashing occurs. If so, reduce the gas flow and blow droplets on the reaction tube walls back into the main body of the solution
		The polymerization solution might have been diluted by too much residual moisture on the sample (Step 17)	Because the volume of polymerization solution necessary to cover a cell culture sample on an 18-mm coverslip is very small (typically 50–60 μl), even relatively small amounts of PBS left adhering to the coverslip can dilute the polymerization solution and thus reduce the extent of DMAA and sodium acrylate cross-linking, resulting in an incompletely polymerized gel. Use a thin tissue to remove as much of the PBS adhering to the sample coverslip as possible, and even consider brief air-drying to reduce moisture
		The temperature might be too high or the polymerization time was too short	Polymerization should ideally be carried out at $20\text{--}25^{\circ}\text{C}$. Higher temperatures can inhibit the polymerization reaction. This is an important difference from the classic 4 \times gel, which polymerizes at 37°C . Polymerization should generally be complete after 2–3 h if the gel was prepared well. Longer polymerization times (up to 24 h) can compensate for this problem, but this is an indication of nonideal polymerization conditions. Gels that are not hardened after 2–3 h can harden with this additional polymerization time and can also expand, but tears in the gel during expansion due to reduced mechanical toughness are common in this case
22	The gel did not remain on the top coverslip of the chamber, but instead remained stuck to the original sample coverslip	If the humidified chamber becomes too dry, this often happens	This is no serious problem, as the gel can be transferred to the digestion chamber on the original sample coverslip as well. Simply remove the top coverslip of the gelation chamber with a razor blade, as usual, and then leverage the sample coverslip off the microscopy slide to transfer it
24	The gel sticks to the walls of the well and cannot be removed from the coverslip	The gel expanded during digestion and thus becomes stuck by adhesion to the plastic	This is perfectly normal and no cause for concern. Remove the gel by gently scraping it out of the well and directly into the expansion chamber with a metal or plastic spatula. Usually, however, with some practice, it should be possible to remove the gel by gripping the gel and the coverslip with forceps; if polymerization was successful, the gel will be stable enough to tolerate this (Fig. 5)
25	The gel was sucked into the pipette or vacuum pump	This can happen because the gel is difficult to see in the water (it becomes completely transparent)	By gently shaking the expansion chamber by hand and looking against reflected light, it is often possible to locate the gel. If the gel cannot be located at all, place the pipette at the rim of the chamber and start to remove the ddH_2O very slowly, all the while moving the pipette around the edge of the chamber. The gel will be sucked in the direction of the water flow, so altering this direction continuously by moving the pipette around the outer rim of the chamber helps to avoid sucking in the gel
28	The sample focus cannot be located	The gel might be flipped with the sample facing away from the objective	Most objectives with a high magnification have too short a working distance to focus through the thickness of the entire gel. Flip the gel around by gently transferring it onto a thin plastic sheet (e.g., the cut-out bottom of a weighing pan), turning the imaging chamber upside down on it, and flipping the assembly. Most 10 \times and 20 \times objectives allow focusing through the entire gel. Imaging depth can be increased by matching the refractive index of the gel to the oil used for objective immersion, i.e., in a sucrose solution ⁴⁶ ; this, however, sacrifices some expansion factor, and thus resolution
	The sample cannot be located at all	The NA of the objective used might be too low, collecting too little light from the sample	Higher-magnification objectives (60 \times or 100 \times) usually have a higher NA, enabling them to collect more light, which makes it easier to visualize the sample. Also, focusing with a high-sensitivity camera rather than the eyepiece can help with particularly dim samples. This can be especially helpful for emission wavelengths to which the human eye has poor sensitivity, i.e., in the red and far-red spectral regions
29	It is not possible to take large overview images on the available microscope setups	Slide scanners or microscopes with a semi-automated stage and stitching function are not available	Take several images at the lowest magnification possible in the center of the coverslip. The center of the sample is easiest to find again after expansion, as it is not affected by rotations of the gel
30	Distortions or ruptures in the sample persist after following all other steps and	Distortions and ruptures can often be attributed to the same cause: insufficient anchoring. This	Reducing the reaction time for the fixation or switching to a less harsh cross-linking fixation agent (i.e., PFA instead of glutaraldehyde,

Table continued

Table 3 (continued)

Step	Problem	Possible reason	Solution
	suggestions on immunostaining, anchoring, polymerization, and digestion detailed in this protocol	<p>can be due to reduced availability of primary amines after fixation (Step 1). Most chemical fixatives that modify the sample covalently, such as PFA or glutaraldehyde, attack primary amine groups. These are the same groups that are later attacked by Acryloyl-X or MA-NHS during anchoring. This is likely to result in distortions in less mechanically tough samples but will also result in ruptures in mechanically tougher samples</p> <p>Distortions and ruptures can often be attributed to the same cause: insufficient anchoring. This can be due to reduced reactivity of the anchoring reagent from improper storage (Step 9). This is likely to result in distortions in mechanically less tough samples but will also result in ruptures in mechanically tougher samples</p> <p>Distortions and ruptures can often be attributed to the same cause: insufficient anchoring (Step 10). This can be due to reduced reactivity of the anchoring reagent from non-optimized anchoring conditions. This is likely to result in distortions in mechanically less tough samples, but will also result in ruptures in mechanically tougher samples. This is a particular problem in tissue slices^{3,2}, but even dense, multilayered cell cultures, such as primary hippocampal neuron cultures, sometimes show ruptures (Fig. 2c, left, arrowheads) with anchoring in PBS at pH 7.4</p> <p>The polymerization solution might have been diluted by too much residual moisture in the sample (Step 17)</p> <p>Distortions and ruptures can often be attributed to the same cause: insufficient homogenization. The reactivity of proteinase K might be less than expected (Step 21)</p> <p>Distortions and ruptures can often be attributed to the same cause: insufficient homogenization. The classic digestion solution is not optimized for maintaining activity of proteinase K for long periods of time at high temperatures (Step 23)</p>	<p>glyoxal⁶⁸ instead of PFA) or, where compatible with the intended labeling, a fixation agent that does not introduce cross-links (e.g., methanol) can alleviate this problem</p> <p>Order new Acryloyl-X and make a new stock solution. Take care not to let the Acryloyl-X come into contact with water. Store it in a desiccated chamber or in an airtight box with silica beads; store it at -20°C to reduce the chance of it reacting with residual water and do not store it for prolonged periods of time (usually 1–3 months) to minimize the risk. Alternatively, MA-NHS can be used as an anchoring reagent instead of Acryloyl-X, as described³. Acryloyl-X and MA-NHS are functionally equivalent, and thus will probably not show substantial differences, but in the case that Acryloyl-X does not yield the expected results, MA-NHS can be tried</p> <p>The original protocols suggest performing anchoring in PBS^{28,35} at around pH 7.0–7.4, or in MES-based saline buffer³⁵ (MBS; 100 mM MES + 150 mM NaCl) at pH 6.0. However, the NHS chemistry reaction of succinimidyl (Acryloyl-X) and primary amine (lysine residues in proteins of the sample) is known to be more efficient at pH 8.3, e.g., in bicarbonate buffers (Fig. 2c). The adjusted anchoring solution given in this protocol (see Reagent setup)³² accounts for this and should be tested as an alternative to PBS at pH 7.0–7.4 or MBS at pH 6.0</p> <p>If there is residual local moisture in some parts of the sample, this may affect the homogeneity of the gel network during polymerization. We recommend briefly air-drying the sample before applying the gel to remove all residual moisture and prevent dilution of the polymerization solution</p> <p>Proteinase K comes in variable quality and variable activity levels, and can also lose activity during storage. The proteinase K specified here in Materials is usually of uniformly high quality and can be stored at 0°C for at least 6 months without appreciable loss of activity. If a loss of activity is suspected, change the proteinase K stock</p> <p>Proteinase K requires Ca^{2+} ions to function at maximum activity for prolonged periods of time at high temperatures, where the enzyme is most active (50°C)⁶¹. In the classic digestion buffer, Ca^{2+} ions are excluded and EDTA is added. The reason for this is most likely an adaptation of the digestion buffer from previous applications of proteinase K, in which proteins should be digested while maintaining DNA or RNA, which required the removal of Ca^{2+} to inactivate nucleases. In immunostaining expansion microscopy, however, DNA or RNA preservation is usually not a consideration and Ca^{2+} can be added and EDTA removed. This is reflected in the adjusted digestion buffer recipe given in the Materials section</p>
	Structural preservation of target structures seems poor	This can be due to inadequate fixation (Step 1). Target structures can also appear to have poor structural preservation due to discontinuous labeling (Step 4). In particular, if tears in the target structures are large, this can also be due to problems in anchoring or homogenization later in the protocol (during Steps 10 and 23; see further troubleshooting advice for Step 30 in this table)	This can be improved by selecting fixation protocols that are optimized for particular target structures. For preservation of cytoskeletal elements, such as tubulin, two alternatives are useful: either 100% (wt/wt) methanol at -20°C for 20 min, or 1 min of 0.3% (vol/vol) glutaraldehyde in extraction buffer at 37°C , followed by 10 min of 2% (vol/vol) glutaraldehyde in cytoskeleton buffer at room temperature ^{19,20}
	Target structures are labeled discontinuously	This can be due to poor probe coverage of the target structures during immunostaining (Step 4)	Coverage of dense and continuous target structures with imaging probes can be incomplete due to steric hindrance, limited epitope accessibility, low affinity of probes, denaturation of epitopes, and so on. This is a problem not specific to expansion microscopy but that is encountered in all super-resolution methods ^{14,52} . This problem can sometimes be addressed by increasing probe concentration or extending labeling time. If you encounter problems such as this, consult specialized guides dealing with the target structures of interest
	The fluorescence signal is extremely dim after expansion	This can be due to poor antibody labeling of the proteins of interest during immunostaining (Step 4)	An increase in labeling intensity can be achieved by any or all of the following measures: (i) increase the antibody concentration, (ii) test different antibodies, (iii) perform the primary antibody incubation overnight at 4°C , or (iv) include an antigen retrieval step after fixation and before the immunostaining (e.g., 100 mM sodium citrate for 30 min at 80°C)
	Signal-to-noise ratio is reduced after steps have been taken to increase labeling intensity	Increasing labeling intensity can often result in increased background, e.g., after increased labeling times or antibody concentrations (Step 7)	Apply stringency washes to remove unspecific background signal. For these, perform another three washes with high-salt PBS, followed by two washes with PBS to remove the increased salt concentration from the sample
	The sample appears extremely dim after expansion	This may be due to insufficiently dense anchoring (Step 10), leading to reduced retention of peptide fragments with an	Anchoring and homogenization must be balanced. Increasing anchoring efficiency can increase fluorophore retention, as can reducing digestion times. In addition, using the adjusted anchoring solution may improve

Table continued

Table 3 (continued)

Step	Problem	Possible reason	Solution
	Homogenization appears too strong or too weak, i.e., the signal is greatly reduced or the sample is severely damaged	<p>accompanying loss of fluorophores after homogenization</p> <p>Proteinase K may not always be the ideal agent for achieving homogenization (Step 21)</p>	<p>the outcome. Anchoring and homogenization have to be balanced against each other for each type of sample (Fig. 2)</p> <p>Proteinase K is a very promiscuous proteolytic enzyme, cutting after aliphatic and aromatic amino acids. Alternative proteinases for weaker³⁵ and additional³⁶ digestion have been proposed as well, and can be considered if proteinase K does not produce the expected results. Specifically, Lys-C results in a better preservation of fluorescent proteins³⁵, whereas adding chitinase and collagenase can digest even <i>Drosophila</i> larva cuticles³⁶. Alternatively, a completely proteinase-free approach can be attempted: autoclaving of the gel for unfolding proteins by denaturation³⁵</p>
	The sample drifts during imaging	The sample is not fixed but can move on the film of water adhering to it	Remove as much excess water as possible before imaging (Fig. 6e). If this is done thoroughly enough, drift should be minimal to nonexistent. Allowing the gel to settle into a stable position for a few minutes after placing it into the imaging chamber can further reduce drift. Alternative suggestions include using poly-L-lysine (PLL)-coated coverslips or embedding the gel in low-melt agarose ^{35,40} , but such measures are usually unnecessary when excess water is removed thoroughly
	The image is blurry	This can be caused by a mismatch of objective and coverslip thickness used in the imaging chamber, a wrongly set correction collar on the objective, or a mismatched immersion medium for the objective	Check the specifications for your objective, and adjust all parameters accordingly. A widely used standard for oil objectives is the use of no. 1.5 coverslips with an immersion medium with a refractive index of 1.518. However, take care to precisely match the two factors (coverslip thickness and refractive index of the immersion medium) to the specifications of any objective you are using, to obtain the best results
	The expected resolution (25 nm for X10) is not reached, despite the expansion factor being as expected	The maximum attainable resolution will not be reached during imaging if the NA of the objective is insufficient. In addition, the spatial sampling of the sample might be inadequate	Resolution is determined by the formula $d = \lambda / (2 \times \text{NA})$, where d is the resolution, λ is the wavelength, and NA is the numerical aperture. To increase resolution, use higher-NA objectives. In addition, the Nyquist criterion for spatial sampling should be taken into account. If the pixel size is too large, maximum resolution will not be achieved
	The image quality is good at the surface of the sample, but degrades deeper in the sample	Achievable imaging depth is degraded when there is a mismatch between the refractive indices of the sample and the immersion medium for which the objective is designed	The refractive index of the expansion gels is close to that of water, of which the gel largely consists after expansion. Oil immersion is poorly matched to this. Therefore, in such samples, oil objectives offer superior performance due to higher NA only within the first few micrometers from the coverslip, whereas deeper in the sample, their focusing and signal collection performance quickly becomes inferior to water-immersion objectives due to spherical aberration ⁵⁴ . To obtain higher sample penetration, switch to appropriate water-immersion objectives, or, alternatively, consider glycerol- or silicone-oil objectives. It is also possible to image the expanded sample after buffer exchange from ddH ₂ O to ddH ₂ O supplemented with sucrose, to better match the refractive index of commonly used immersion oils (although this prevents the gel from reaching its maximum expansion factor, thus reducing resolution) ⁴⁶
31C(iii)	It is impossible to match pre- and post-expansion images	The resolution of the pre- and the post-expansion image is too different to identify the same regions easily, or the imaged overview regions do not overlap	Imaged with the same objective, the resolution will be ten times better with X10 after expansion compared to before expansion. Computationally reducing the resolution of the post-expansion image helps to make the structures look more similar, easing alignment. The Python script enclosed with this paper (Supplementary Data 1) achieves this via image smoothening with a Gaussian function of an approximate width of the objective point-spread function times the expansion factor. To increase the likelihood of finding an alignment, increase the size of the pre- and post-expansion overview images
32	The distortions are severe	This might be explained by a number of issues that occurred in previous steps, as detailed in the troubleshooting advice in this table for Step 30 (with the original issue probably occurring during Step 1, 9, 10, 21, or 23)	See previous troubleshooting advice in this table for Step 30

Timing

The protocol presented here can be divided into seven stages (labeling, anchoring, polymerization, homogenization, expansion, imaging, and validation), all of which taken together will require ~3 d to complete, with a total of ~8 h of bench and imaging time for one sample (Fig. 1):

Steps 1–8, labeling via standard immunostaining techniques: 4–5 h, with 2–3 h of bench time

Steps 9–11, anchoring: at least 6 h, typically performed as an overnight step, with <15 min of bench time

Steps 12–20, polymerization: 2–3 h, with ~1 h of bench time

Steps 21–23, homogenization: at least 12 h, typically performed as an overnight step, with <15 min of bench time

Steps 24 and 25, expansion: 1–2 h, with <1 h of bench time

Steps 26–30, imaging: timing can vary widely from sample to sample and depending on the specific experimental question, but typically will be in the range of 2–3 h

Steps 31 and 32, validation: variable, but typically 30 min, which is mostly processing time when using the script provided here

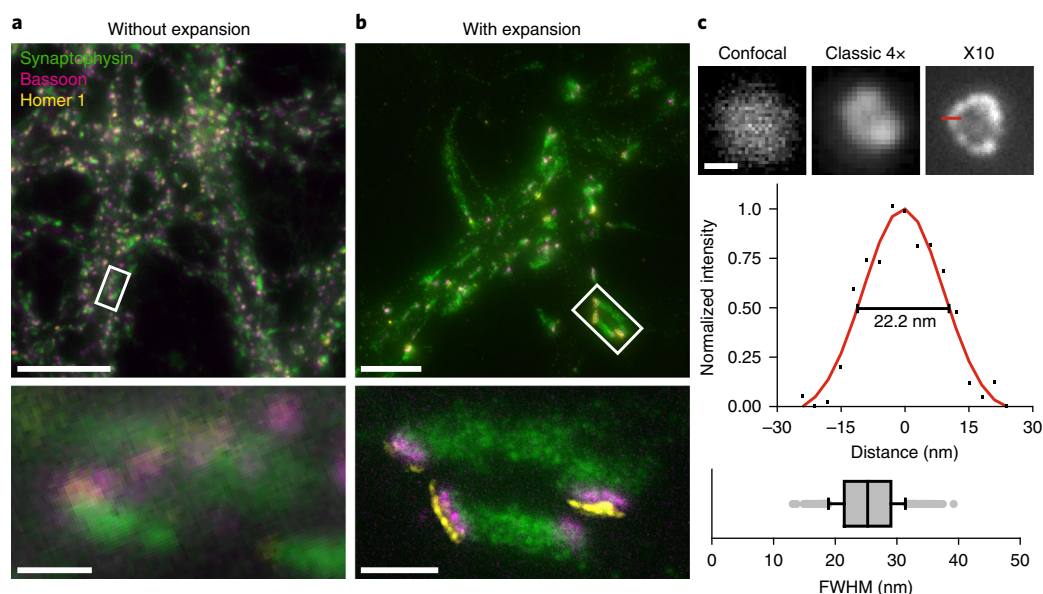


Fig. 8 | Expected results, exemplary images of samples before and after expansion. **a**, Exemplary overview image (top) of neuronal cell cultures stained for synaptophysin (green), a synaptic vesicle marker; Bassoon (magenta), an active zone protein; and Homer 1 (yellow), a postsynaptic density protein. The sample was imaged on a wide-field microscope without expansion. The boxed region with individual synapses is magnified in the bottom panel. Scale bars, top, 10 μm ; bottom, 1 μm . **b**, Exemplary images of synapses labeled as in **a**, but after X10 expansion. The overview image (top) is a maximum-intensity projection of a 77-slice z-stack spanning 15 μm (200-nm step size) in terms of physical size, or $\sim 1.5 \mu\text{m}$ (20-nm step size) downsampled to the sample's size before expansion. The magnified view below shows a maximum-intensity projection of the three slices of best focus for the boxed region. The images in **a** and **b** were taken on the same microscope, at the same magnification and with the same objective (100 \times , NA 1.4). Expansion factor: 9.5 \times . Scale bars, top, 2 μm ; bottom, 500 nm. **c**, Exemplary images of peroxisomes labeled for the membrane protein Pmp70, imaged with confocal microscopy (left), classic fourfold expansion microscopy (center), and X10 microscopy (right). The graph below the images shows the best Gaussian fit through the red line in the X10 image. The full width at half maximum (FWHM) of this line scan was used to approximate the resolution after expansion with X10. The box plot below shows a quantification of FWHM measurements based on such line scans ($n = 653$ line scans across peroxisomes from two independent experiments). The data are represented as a box plot with median (horizontal line) and upper and lower quartile boundaries (box range), plus 1.5 \times the interquartile range (whiskers) and outliers (dots). Expansion factors: 3.8 \times for classic fourfold expansion microscopy and 9.5 \times for X10. Scale bar: 100 nm (applies to all panels in **c**). **c** adapted with permission from Truckenbrodt et al.³² under a Creative Commons Attribution 4.0 license (<https://creativecommons.org/licenses/by/4.0/legalcode>).

Anticipated results

If all steps in the protocol have been followed carefully, the sample should expand approximately tenfold for the X10 gel, show distortions of <100–200 nm root mean square error over a distance of $\sim 5 \mu\text{m}$, display no ruptures, and be sufficiently bright to observe under a suitable microscope³². The expected resolution is $\sim 25 \text{ nm}$ for X10 microscopy when imaged with an epifluorescence or confocal microscope and a high-NA objective lens. By contrast, if the classic 4 \times gel were used in the appropriate steps of the Procedure, expansion would be around fourfold and the attained resolution would be $\sim 70 \text{ nm}$ ²⁸. Figure 8 shows exemplary images of data quality to expect when the X10 gel is imaged on an epifluorescence microscope. Here, dissociated neuron cultures are stained with antibodies for synaptophysin, Bassoon, and Homer 1, highlighting synaptic vesicles, presynaptic active zones, and postsynaptic densities, respectively. With X10 expansion microscopy, individual synaptic vesicles and the nanoscale alignment between pre- and post-synapse can be discerned on a regular wide-field microscope. In the non-expanded conventional image, these structures and organizational features cannot be recognized.

Figure 7 provides a visualization of the distortions that are typically present in this type of sample after expansion evaluated with the Python scripts provided with this paper. The scripts find the best global fit with respect to position and rotation of the pre- and post-expansion images, and the vector field generated gives the local offsets between the same pre- and post-expansion structures. Note that, depending on the imaging conditions and size of the image (small region imaged with high-NA objective versus large region imaged with low-NA objective), distortions on various spatial scales can be evaluated. To obtain accurate scaling of measurement results, it is imperative to determine the expansion factor for each individual sample, as the precise expansion factor shows variation (10 ± 0.27 for the data presented in Fig. 7d).

The experimental data in Fig. 8 represents a high-quality experimental outcome, featuring both high resolution and high signal-to-background ratio. Without expansion (Fig. 8a), even the separation of pre- and postsynaptic markers is difficult to perceive, but with expansion, the separation is readily apparent (Fig. 8b). The nanoscale alignment between these presynaptic active zone and postsynaptic density constituents can now be discerned. Individual densely packed synaptic vesicles (40-nm diameter) can also be visualized.

It is important to note that anchoring and digestion are based on chemical reactions that never reach perfect efficiency. Even under optimized conditions, not every anchoring site will become anchored and not every digestion site will become cut. Samples are also different in mechanical toughness, even different kinds of cell culture. The primary hippocampal neuronal cultures used herein are relatively complex multilayered cultures consisting of neurons and several types of glia, adding to the mechanical toughness as compared to that of most single-layered cultures of cell lines. Thus, improving sample preparation relies on increasing the efficiency of anchoring and homogenization (Fig. 2a); optimization is necessary for any type of sample and should be appropriate to the problems encountered (Table 2). The data in Fig. 2 show two instances of failed experiments and measures that can be attempted to resolve such issues. In the first example in Fig. 2b, the sample fragmented due to insufficient mechanical homogenization. Ruptures are prevalent in the condition of only moderate homogenization (Fig. 2b, left). Performing homogenization in an optimized digestion buffer that contains Ca^{2+} ions to stabilize proteinase K during prolonged digestion has the benefit of avoiding ruptures and distortions, especially in mechanically tough samples such as multilayered cell cultures or tissue slices³². However, an optimized digestion also can have the side effect of reducing the number of fluorophores that are available after homogenization by increasing the fragmentation of peptides. In the example shown in Fig. 2b, in the right-hand overview image, elevated digestion paired with moderate anchoring led to a high loss of fluorophores. Loss in intensity can be partially compensated for by adjusting the imaging parameters (e.g., exposure time, light intensity, gain), as shown in the magnified panels of both conditions (Fig. 2b). Here, the limit for increasing digestion is given by a decline in signal-to-noise ratio once fluorophore loss becomes severe. It is important to note that none of the conditions shown in Fig. 2a is automatically superior to the others, but optimization is required to tailor the anchoring and homogenization to any specific type of sample to obtain optimal results. At the same time, the trade-off between increased digestion and signal amplitude becomes clear. In the right-hand panel in Fig. 2b, some signal was lost due to increased digestion, but the overall signal-to-background ratio was acceptable. Increasing digestion further would have resulted in unacceptably high loss of fluorophores here. In Fig. 2c, an alternative route to ensuring sample integrity after expansion was followed, namely to increase anchoring, which in addition promotes fluorophore retention. Ruptures that sometimes occur after anchoring in PBS at pH 7.4 after approximately tenfold expansion (Fig. 2c, left) are usually completely absent when using an optimized protocol, in which anchoring is performed in carbonate buffer (150 mM NaHCO_3) at pH 8.3 (Fig. 2c, right).

Reporting Summary

Further information on experimental design is available in the Nature Research Reporting Summary linked to this article.

Code availability

The code used and described in this paper is available as Supplementary Data 1. Additional advice on how to use it can be obtained from the authors upon reasonable request.

Data availability

All data shown in this paper are available from the authors upon reasonable request.

References

1. Hell, S. W. & Wichmann, J. Breaking the diffraction resolution limit by stimulated emission: stimulated-emission-depletion fluorescence microscopy. *Opt. Lett.* **19**, 780–782 (1994).
2. Klar, T. A. & Hell, S. W. Subdiffraction resolution in far-field fluorescence microscopy. *Opt. Lett.* **24**, 954–956 (1999).
3. Betzig, E. et al. Imaging intracellular fluorescent proteins at nanometer resolution. *Science* **313**, 1642–1645 (2006).

4. Rust, M. J., Bates, M. & Zhuang, X. Sub-diffraction-limit imaging by stochastic optical reconstruction microscopy (STORM). *Nat. Methods* **3**, 793–795 (2006).
5. Hess, S. T., Girirajan, T. P. K. & Mason, M. D. Ultra-high resolution imaging by fluorescence photoactivation localization microscopy. *Biophys. J.* **91**, 4258–4272 (2006).
6. Heilemann, M. et al. Subdiffraction-resolution fluorescence imaging with conventional fluorescent probes. *Angew. Chem. Int. Ed. Engl.* **47**, 6172–6176 (2008).
7. Fölling, J. et al. Fluorescence nanoscopy by ground-state depletion and single-molecule return. *Nat. Methods* **5**, 943–945 (2008).
8. Giannone, G. et al. Dynamic superresolution imaging of endogenous proteins on living cells at ultra-high density. *Biophys. J.* **99**, 1303–1310 (2010).
9. Jungmann, R. et al. Single-molecule kinetics and super-resolution microscopy by fluorescence imaging of transient binding on DNA origami. *Nano Lett.* **10**, 4756–4761 (2010).
10. Sharonov, A. & Hochstrasser, R. M. Wide-field subdiffraction imaging by accumulated binding of diffusing probes. *Proc. Natl. Acad. Sci. USA* **103**, 18911–18916 (2006).
11. Gustafsson, M. Surpassing the lateral resolution limit by a factor of two using structured illumination microscopy. *J. Microsc.* **198**, 82–87 (2000).
12. Gustafsson, M. Nonlinear structured-illumination microscopy: wide-field fluorescence imaging with theoretically unlimited resolution. *Proc. Natl. Acad. Sci. USA* **102**, 13081–13086 (2005).
13. Fornasiero, E. F. & Opazo, F. Super-resolution imaging for cell biologists. *Bioessays* **37**, 436–451 (2015).
14. Saka, S. & Rizzoli, S. O. Super-resolution imaging prompts re-thinking of cell biology mechanisms: selected cases using stimulated emission depletion microscopy. *Bioessays* **34**, 386–395 (2012).
15. Baddeley, D. & Bewersdorf, J. Biological insight from super-resolution microscopy: what we can learn from localization-based images. *Annu. Rev. Biochem.* **87**, 965–989 (2018).
16. Schermelleh, L., Heintzmann, R. & Leonhardt, H. A guide to super-resolution fluorescence microscopy. *J. Cell Biol.* **190**, 165–175 (2010).
17. Dani, A., Huang, B., Bergan, J., Dulac, C. & Zhuang, X. Superresolution imaging of chemical synapses in the brain. *Neuron* **68**, 843–856 (2010).
18. Sahl, S. J., Hell, S. W. & Jakobs, S. Fluorescence nanoscopy in cell biology. *Nat. Rev. Mol. Cell Biol.* **18**, 685–701 (2017).
19. Xu, K., Zhong, G. & Zhuang, X. Actin, spectrin, and associated proteins form a periodic cytoskeletal structure in axons. *Science* **339**, 452–456 (2013).
20. D’Este, E. et al. Subcortical cytoskeleton periodicity throughout the nervous system. *Sci. Rep.* **6**, 22741 (2016).
21. Sidenstein, S. C. et al. Multicolour multilevel STED nanoscopy of actin/spectrin organization at synapses. *Sci. Rep.* **6**, 26725 (2016).
22. Hoopmann, P. et al. Endosomal sorting of readily releasable synaptic vesicles. *Proc. Natl. Acad. Sci. USA* **107**, 19055–19060 (2010).
23. Westphal, V. et al. Video-rate far-field optical nanoscopy dissects synaptic vesicle movement. *Science* **320**, 246–249 (2008).
24. Willig, K. I., Rizzoli, S. O., Westphal, V., Jahn, R. & Hell, S. W. STED microscopy reveals that synaptotagmin remains clustered after synaptic vesicle exocytosis. *Nature* **440**, 935–939 (2006).
25. Chojnacki, J. et al. Maturation-dependent HIV-1 surface protein redistribution revealed by fluorescence nanoscopy. *Science* **338**, 524–528 (2012).
26. Kittel, R. J. et al. Bruchpilot promotes active zone assembly, Ca^{2+} channel clustering, and vesicle release. *Science* **312**, 1051–1054 (2006).
27. Böhme, M. A. et al. Active zone scaffolds differentially accumulate Unc13 isoforms to tune Ca^{2+} channel-vesicle coupling. *Nat. Neurosci.* **19**, 1311–1320 (2016).
28. Chen, F., Tillberg, P. W. & Boyden, E. S. Expansion microscopy. *Science* **347**, 543–548 (2015).
29. Gao, R., Asano, S. M. & Boyden, E. S. Q&A: expansion microscopy. *BMC Biol.* **15**, 50 (2017).
30. Cho, I., Seo, J. Y. & Chang, J. Expansion microscopy. *J. Microsc.* **271**, 123–128 (2018).
31. Chang, J. B. et al. Iterative expansion microscopy. *Nat. Methods* **14**, 593–599 (2017).
32. Trukenbrodt, S. et al. X10 expansion microscopy enables 25 nm resolution on conventional microscopes. *EMBO Rep.* **19**, e45836 (2018).
33. Chozinski, T. J. et al. Expansion microscopy with conventional antibodies and fluorescent proteins. *Nat. Methods* **13**, 485–488 (2016).
34. Zhao, Y. et al. Nanoscale imaging of clinical specimens using pathology-optimized expansion microscopy. *Nat. Biotechnol.* **35**, 757–764 (2017).
35. Tillberg, P. W. et al. Protein-retention expansion microscopy of cells and tissues labeled using standard fluorescent proteins and antibodies. *Nat. Biotechnol.* **34**, 987–992 (2016).
36. Jiang, N. et al. Super-resolution imaging of *Drosophila* tissues using expansion microscopy. *Mol. Biol. Cell* **29**, 1413–1421 (2018).
37. Freifeld, L. et al. Expansion microscopy of zebrafish for neuroscience and developmental biology studies. *Proc. Natl. Acad. Sci. USA* **114**, E10799–E10808 (2017).
38. Cahoon, C. K. et al. Superresolution expansion microscopy reveals the three-dimensional organization of the *Drosophila* synaptonemal complex. *Proc. Natl. Acad. Sci. USA* **114**, E6857–E6866 (2017).
39. Cipriano, B. H. et al. Superabsorbent hydrogels that are robust and highly stretchable. *Macromolecules* **47**, 4445–4452 (2014).

40. Asano, S. M. et al. Expansion microscopy: protocols for imaging proteins and RNA in cells and tissues. *Curr. Protoc. Cell Biol.* **80**, e56 (2018).
41. Wang, G., Moffitt, J. R. & Zhuang, X. Multiplexed imaging of high-density libraries of RNAs with MERFISH and expansion microscopy. *Sci. Rep.* **8**, 4847 (2018).
42. Chen, F. et al. Nanoscale imaging of RNA with expansion microscopy. *Nat. Methods* **13**, 679–684 (2016).
43. Gao, R. et al. Cortical column and whole-brain imaging with molecular contrast and nanoscale resolution. *Science* **363**, eaau8302 (2019).
44. Halpern, A. R., Alas, G. C. M., Chozinski, T. J., Paredes, A. R. & Vaughan, J. C. Hybrid structured illumination expansion microscopy reveals microbial cytoskeleton organization. *ACS Nano* **11**, 12677–12686 (2017).
45. Wang, Y. et al. Combined expansion microscopy with structured illumination microscopy for analyzing protein complexes. *Nat. Protoc.* **13**, 1869–1895 (2018).
46. Gao, M. et al. Expansion stimulated emission depletion microscopy (ExSTED). *ACS Nano* **12**, 4178–4185 (2018).
47. Gambarotto, D. et al. Imaging beyond the super-resolution limits using ultrastructure expansion microscopy (U-ExM). *Nat. Methods* **16**, 71–74 (2019).
48. Tong, Z. et al. Ex-STORM: expansion single molecule super-resolution microscopy. Preprint at <https://www.biorxiv.org/content/10.1101/374140v1> (2016).
49. Ku, T. et al. Multiplexed and scalable super-resolution imaging of three-dimensional protein localization in size-adjustable tissues. *Nat. Biotechnol.* **34**, 973–981 (2016).
50. Murakami, T. C. et al. A three-dimensional single-cell-resolution whole-brain atlas using CUBIC-X expansion microscopy and tissue clearing. *Nat. Neurosci.* **21**, 625–637 (2018).
51. Mikhaylova, M. et al. Resolving bundled microtubules using anti-tubulin nanobodies. *Nat. Commun.* **6**, 7933 (2015).
52. Maidorn, M., Rizzoli, S. O. & Opazo, F. Tools and limitations to study the molecular composition of synapses by fluorescence microscopy. *Biochem. J.* **473**, 3385–3399 (2016).
53. Ries, J., Kaplan, C., Platonova, E., Eghlidi, H. & Ewers, H. A simple, versatile method for GFP-based super-resolution microscopy via nanobodies. *Nat. Methods* **9**, 582–584 (2012).
54. Hell, S., Reiner, G., Cremer, C. & Stelzer, E. H. K. Aberrations in confocal fluorescence microscopy induced by mismatches in refractive index. *J. Microsc.* **169**, 391–405 (1993).
55. Wegel, E. et al. Imaging cellular structures in super-resolution with SIM, STED and localisation microscopy: a practical comparison. *Sci. Rep.* **6**, 27290 (2016).
56. Sahl, S. J. & Moerner, W. E. Super-resolution fluorescence imaging with single molecules. *Curr. Opin. Struct. Biol.* **623**, 778–787 (2013).
57. Hell, S. W. Far-field optical nanoscopy. *Science* **316**, 1153–1158 (2007).
58. Banker, G. A. & Cowan, W. M. Rat hippocampal neurons in dispersed cell culture. *Brain Res.* **126**, 397–425 (1977).
59. Kaech, S. & Banker, G. Culturing hippocampal neurons. *Nat. Protoc.* **1**, 2406–2415 (2006).
60. Truckenbrodt, S. et al. Newly produced synaptic vesicle proteins are preferentially used in synaptic transmission. *EMBO J.* **37**, e98044 (2018).
61. Bajorath, J., Hinrichs, W. & Saenger, W. The enzymatic activity of proteinase K is controlled by calcium. *Eur. J. Biochem.* **176**, 441–447 (1988).
62. Glynn, M. W. & McAllister, A. K. Immunocytochemistry and quantification of protein colocalization in cultured neurons. *Nat. Protoc.* **1**, 1287–1296 (2006).
63. Schneider Gasser, E. M. et al. Immunofluorescence in brain sections: simultaneous detection of presynaptic and postsynaptic proteins in identified neurons. *Nat. Protoc.* **1**, 1887–1897 (2006).
64. Richter, K. N. et al. Glyoxal as an alternative fixative to formaldehyde in immunostaining and super-resolution microscopy. *EMBO J.* **37**, 139–159 (2018).
65. Laftah, W. A., Hashim, S. & Ibrahim, A. N. Polymer hydrogels: a review. *Polym. Plast. Technol. Eng.* **50**, 1475–1486 (2011).
66. Osada, Y., Gong, J. & Tanaka, Y. Polymer gels. *J. Macromol. Sci. Part C Polym. Rev.* **1**, 339–366 (2012).
67. Zohuriaan-Mehr, M. J. & Kabiri, K. Superabsorbent polymer materials: a review. *Iran. Polym. J.* **17**, 451–477 (2008).
68. Lee, W. & Wu, R. Superabsorbent polymeric materials. 1. Swelling behaviors of crosslinked poly(sodium acrylate-co-hydroxyethyl methacrylate) in aqueous salt solution. *J. Appl. Polym. Sci.* **62**, 1099–1114 (1996).

Acknowledgements

We thank E. De Gaulejac and D. Lorenz for critically reading the manuscript. We thank S. Kabatas for helpful discussions. S.T. has received funding, as an ISTplus Fellow, from the European Union's Horizon 2020 Research and Innovation Programme under Marie Skłodowska-Curie grant agreement no. 754411. J.G.D. gratefully acknowledges funding by the Austrian Science Fund (FWF; I 3600-B27). This work was further supported by grants to S.O.R. from the European Research Council (ERC-2013-CoG NeuroMolAnatomy) and the Deutsche Forschungsgemeinschaft (DFG; SFB1286/Z03).

Author contributions

S.T., J.G.D., and S.O.R. prepared the manuscript. S.T. prepared the figures. S.T. performed the experiments and imaging. C.S. wrote the Python Anaconda scripts provided here for alignment of pre- and post-expansion images, expansion factor determination, and distortion analysis.

Competing interests

The authors declare no competing interests.

Additional information

Supplementary information is available for this paper at <https://doi.org/10.1038/s41596-018-0117-3>.

Reprints and permissions information is available at www.nature.com/reprints.

Correspondence and requests for materials should be addressed to S.T.

Publisher's note: Springer Nature remains neutral with regard to jurisdictional claims in published maps and institutional affiliations.

Received: 13 August 2018 Accepted: 20 December 2018

Published online: 18 February 2019

Related link**Key reference using this protocol**

Truckenbrodt, S. et al. *EMBO Rep.* **19**, e45836 (2018): <http://embor.embopress.org/content/early/2018/07/09/embr.201845836>

Reporting Summary

Nature Research wishes to improve the reproducibility of the work that we publish. This form provides structure for consistency and transparency in reporting. For further information on Nature Research policies, see [Authors & Referees](#) and the [Editorial Policy Checklist](#).

Statistical parameters

When statistical analyses are reported, confirm that the following items are present in the relevant location (e.g. figure legend, table legend, main text, or Methods section).

n/a Confirmed

- | | | |
|-------------------------------------|-------------------------------------|---------------------------------------------------------------------------------------------------------------------------------------------------------------------------------------------------------------------------------------------------------------------|
| <input type="checkbox"/> | <input checked="" type="checkbox"/> | The <u>exact sample size</u> (<i>n</i>) for each experimental group/condition, given as a discrete number and unit of measurement |
| <input type="checkbox"/> | <input checked="" type="checkbox"/> | An indication of whether measurements were taken from distinct samples or whether the same sample was measured repeatedly |
| <input checked="" type="checkbox"/> | <input type="checkbox"/> | The statistical test(s) used AND whether they are one- or two-sided
<i>Only common tests should be described solely by name; describe more complex techniques in the Methods section.</i> |
| <input checked="" type="checkbox"/> | <input type="checkbox"/> | A description of all covariates tested |
| <input checked="" type="checkbox"/> | <input type="checkbox"/> | A description of any assumptions or corrections, such as tests of normality and adjustment for multiple comparisons |
| <input checked="" type="checkbox"/> | <input type="checkbox"/> | A full description of the statistics including <u>central tendency</u> (e.g. means) or other basic estimates (e.g. regression coefficient) AND <u>variation</u> (e.g. standard deviation) or associated <u>estimates of uncertainty</u> (e.g. confidence intervals) |
| <input checked="" type="checkbox"/> | <input type="checkbox"/> | For null hypothesis testing, the test statistic (e.g. <i>F</i> , <i>t</i> , <i>r</i>) with confidence intervals, effect sizes, degrees of freedom and <i>P</i> value noted
<i>Give P values as exact values whenever suitable.</i> |
| <input checked="" type="checkbox"/> | <input type="checkbox"/> | For Bayesian analysis, information on the choice of priors and Markov chain Monte Carlo settings |
| <input checked="" type="checkbox"/> | <input type="checkbox"/> | For hierarchical and complex designs, identification of the appropriate level for tests and full reporting of outcomes |
| <input checked="" type="checkbox"/> | <input type="checkbox"/> | Estimates of effect sizes (e.g. Cohen's <i>d</i> , Pearson's <i>r</i>), indicating how they were calculated |
| <input type="checkbox"/> | <input checked="" type="checkbox"/> | Clearly defined error bars
<i>State explicitly what error bars represent (e.g. SD, SE, CI)</i> |

Our web collection on [statistics for biologists](#) may be useful.

Software and code

Policy information about [availability of computer code](#)

Data collection

For imaging data collection, we used the commercial Nikon NIS Elements (version 4.20.03) software.

Data analysis

For data analysis, we used ImageJ (version 1.47v) and custom-written Python (version 3.6) Anaconda (version 5.2) routines (code enclosed with the manuscript).

For manuscripts utilizing custom algorithms or software that are central to the research but not yet described in published literature, software must be made available to editors/reviewers upon request. We strongly encourage code deposition in a community repository (e.g. GitHub). See the Nature Research [guidelines for submitting code & software](#) for further information.

Data

Policy information about [availability of data](#)

All manuscripts must include a [data availability statement](#). This statement should provide the following information, where applicable:

- Accession codes, unique identifiers, or web links for publicly available datasets
- A list of figures that have associated raw data
- A description of any restrictions on data availability

All data shown in this manuscript are available from the authors upon reasonable request.

Field-specific reporting

Please select the best fit for your research. If you are not sure, read the appropriate sections before making your selection.

☒ Life sciences ☐ Behavioural & social sciences ☐ Ecological, evolutionary & environmental sciences

For a reference copy of the document with all sections, see [nature.com/authors/policies/ReportingSummary-flat.pdf](https://www.nature.com/authors/policies/ReportingSummary-flat.pdf)

Life sciences study design

All studies must disclose on these points even when the disclosure is negative.

Sample size	No sample-size calculation was performed, as we do not include any statistics in this manuscript.
Data exclusions	No data exclusion took place.
Replication	All data shown here have been reproduced at least three times in the two different labs involved in this study.
Randomization	No specific process of randomization was performed, as there were no parameters in our experiments that necessitated randomization.
Blinding	No blinding was performed as the data we show here illustrates a usually non-blinded optimization process.

Reporting for specific materials, systems and methods

Materials & experimental systems

n/a	Involved in the study
<input checked="" type="checkbox"/>	<input type="checkbox"/> Unique biological materials
<input type="checkbox"/>	<input checked="" type="checkbox"/> Antibodies
<input checked="" type="checkbox"/>	<input type="checkbox"/> Eukaryotic cell lines
<input checked="" type="checkbox"/>	<input type="checkbox"/> Palaeontology
<input type="checkbox"/>	<input checked="" type="checkbox"/> Animals and other organisms
<input checked="" type="checkbox"/>	<input type="checkbox"/> Human research participants

Methods

n/a	Involved in the study
<input checked="" type="checkbox"/>	<input type="checkbox"/> ChIP-seq
<input checked="" type="checkbox"/>	<input type="checkbox"/> Flow cytometry
<input checked="" type="checkbox"/>	<input type="checkbox"/> MRI-based neuroimaging

Antibodies

Antibodies used	<p>primary antibodies</p> <p>anti-Synaptophysin: Synaptic Systems, guinea pig polyclonal, cat. no. 101 004</p> <p>anti-Homer 1: Synaptic Systems, rabbit polyclonal, cat. no. 160 003</p> <p>anti-Bassoon: Enzo, mouse monoclonal, cat. no. SAP7F407</p> <p>secondary antibodies</p> <p>anti-guinea pig: Dianova, donkey polyclonal, cat. no. 706-545-148, conjugated to Alexa Fluor 488</p> <p>anti-rabbit: Invitrogen, goat polyclonal, cat. no. A11035, conjugated to Alexa Fluor 546</p> <p>anti-mouse: Biotium, donkey polyclonal, cat. no. 20124, conjugated to CF633</p>
Validation	<p>Stainings with the antibodies used here corresponded to the staining patterns expected for their target structures (Synaptophysin, synaptic vesicles; Homer 1, post-synaptic densities; Bassoon, pre-synaptic active zones). No further validation was performed by us. For manufacturer validation, see the product pages listed below.</p> <p>anti-Synaptophysin: https://www.sysy.com/products/s-physin1/facts-101004.php</p> <p>anti-Homer 1: https://www.sysy.com/products/homer1/facts-160003.php</p> <p>anti-Bassoon: http://www.enzolifesciences.com/ADI-VAM-PS003/bassoon-monoclonal-antibody-sap7f407/</p>

Animals and other organisms

Policy information about [studies involving animals](#); [ARRIVE guidelines](#) recommended for reporting animal research

Laboratory animals	We obtained primary hippocampal neurons from Wistar rat pups (P1-P2) of mixed gender, bred and maintained at IST Austria (originally sourced from JanvierLabs, Le Genest-Saint-Isle, France).
--------------------	-----------------------------------------------------------------------------------------------------------------------------------------------------------------------------------------------

Wild animals

No wild animals were used in this study.

Field-collected samples

No field-collected samples were used in this study.